Eco-Hydrological Simulation Environment (`echse`)

Documentation of model engines

Author   David Kneis
Affiliation Institute of Earth and Environmental Sciences
            Geo-Ecology Section,
            University of Potsdam, Germany
Contact   david.kneis@uni-potsdam.de

Last update March 15, 2014

Contents

Chapter 1

Introduction

This document is subdivided into three parts each of them adressing a different level of software hierarchy. The relation between the tree parts is depicted by an example in Fig. 1.1.

Part I contains a brief description of hydrological model engines implemented with the **echse** modeling framework. It provides information on the model engine's purpose and lists the important classes (i. e. the types of objects that can be simulated) using references to the part II.

Part II holds a description of the classes, including information on state variables and external inputs, for example.

Part III addresses the mathematical representation of realworld hydrological processes, i. e. the mechanisms that cause the state variables to change their values over time. The concepts described in this part may be used by several of the classes portrayed in part II.
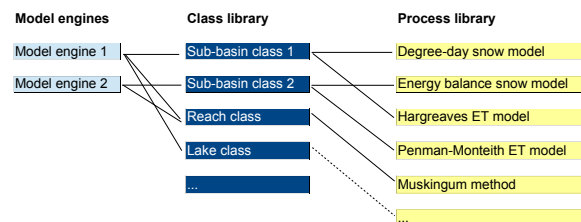
Figure 1.1: *Classes and processes as the basic building blocks of hydrological model engines.*

Part I

Hydrological model engines

Chapter 2

Model engine `hypsoRR`

2.1 Basic facts

The **hypsoRR** model engine was designed for the purpose of flood forecasting, and the verification of ensemble-based flood forecasts in particular.

- It is hydrologocal catchment model engine that simulates all major processes of the hydrological cycle.

- It is a rather simple, conceptual model engine to allow for fast computations. This is important in operational applications, especially when dealing with ensembles.

- The data requirements are adapted to the situation in Germany, where observation data for all major meteorological variables are typically available. However, the concept was also sucessfully applied to basins in Asia and Africa. The full set of variables is required only if snow accumulation/melt is relevant.

- Many concepts are copied from LARSIM (Ludwig and Bremicker, 2006) which is the hydrological model engine currently used for operational forecasting in SW Germany. **hypsoRR** can use most of LARSIM's input data, namely the information in tape12, tape35, etc.

2.2 Classes

The **hypsoRR** model engine currently comprises the classes listes in Table 2.1.

Table 2.1: Classes of the **hypsoRR** model engine.

Class	Details to be found at
Sub-basin	Sec. 3.1
Reach	Sec. 3.2
Minireach	Sec. 3.3
Node classes	Sec. 3.4
Lake	Sec. 3.5
Gage	Sec. 3.6
Rain gage	Sec. 3.7
External inflow	Sec. 3.8

2.3 Selected applications

As of March 2014, **hypsoRR** was set-up and calibrated for the river basins listes in Table 2.2.

Table 2.2: Applications of the **hypsoRR** model engine.

Basin/Gage	Country	km^2
Wilde Weißeritz / Ammelsdorf	Germany	70
Rheraya	Morocco	220
Marikina	Philippines	570
Neckar / Kirchtellinsfurt	Germany	2317
Mahanadi / Mundali	India	135000

Part II

Classes

Chapter 3

Classes for hydrological catchment modeling

3.1 Default sub-basin class

3.1.1 Simulated processes

The class simulates the processes listed in Table 3.1.

The current version of the class does *not* allow for the representation of hydrological response units. Only three classes of land cover are currently distinguished: (1) water surfaces, (2) impervious surfaces, and (3) pervious surfaces, i. e. soil typically covered by vegetation.

3.1.2 Data members

A full list of the data members of the class is provided in Table 3.2. See Kneis (2012b) for an explanation of the abbreviations in the 'type' column.

Table 3.1: Considered processes in the default sub-basin class.

Process	Model concept
Runoff generation	Conceptual four components model (Sec. 5.2)
Runoff concentration	Parallel linear reservoirs (Sec. 6.2)
Evapotranspiration	Potential evapotranspiration after Makkink with crop factors and correction for soil water limitation (Sections 9.4, 9.5.1, and 9.5.2)
Snow storage and melt	Energy balance model (Sec. 4.1)

Table 3.2: *Data members of the default sub-basin class.*

Type	Name	Description	Unit
stateScal	wc	Soil water content (dimensionless, i.e. vol/vol or m/m)	dimensionless
stateScal	vol_surf	Storage volume of the linear reservoir controlling surface runoff retention	m3
stateScal	vol_pref	Storage volume of the linear reservoir controlling preferential flow retention	m3
stateScal	vol_inter	Storage volume of the linear reservoir controlling interflow retention	m3
stateScal	vol_base	Storage volume of the linear reservoir controlling baseflow retention	m3
stateScal	snow_swe	Snow water equivalent	m
stateScal	snow_sec	Energy content of the snow cover	kJ/m2
stateScal	snow_alb	Snow albedo	dimensionless
inputExt	precip_resid	Residuals of precipitation (time series)	mm / time step
inputExt	precip_slope	Slope of the linear model precip ˜ elevation	mm / time step / meter
inputExt	precip_inter	Intercept of the linear model precip ˜ elevation	mm / time step
inputExt	temper_resid	Residuals of air temperature (time series)	degree Celsius
inputExt	temper_slope	Slope of the linear model temperature ˜ elevation	degree Celsius / meter
inputExt	temper_inter	Intercept of the linear model temperature ˜ elevation	degree Celsius
inputExt	apress_resid	Residuals of air pressure (time series)	hPa
inputExt	apress_slope	Slope of the linear model pressure ˜ elevation	hPa / meter
inputExt	apress_inter	Intercept of the linear model pressure ˜ elevation	hPa
inputExt	windsp	Wind speed (time series)	m/s
inputExt	glorad	Short-wave radiation (time series)	W/m2
inputExt	rhumid	Relative humidity (time series)	%
inputExt	clness	Cloudiness (time series)	dimenionless (0...1)
inputExt	lai	Leaf area index	dimensionless
paramNum	area	Surface area of the catchment	m2
paramNum	elev	Representative elevation	m asl
paramNum	frac_noinf	Fraction of the catchment area with impervious surface	dimensionless (0...1)
paramNum	frac_water	Fraction of the catchment area covered by water surfaces	dimensionless (0...1)
paramNum	soildepth	Thickness of the modeled soil column	m
paramNum	wc_max	Maximum value soil water content (water content at saturation)	dimensionless
paramNum	exp_satfrac	Shape parameter, controls the fraction of saturated areas with increasing average saturation	dimensionless
paramNum	thr_surf	Threshold value. Direct runoff above this rate is considered as surface runoff	m/s
paramNum	relsat_inter	Relative filling of soil reservoir above which interflow is generated (threshold)	dimensionless (0...1)
paramNum	rate_inter	Rate of medium-fast runoff generation at soil saturation	m/s
paramNum	rate_base	Rate of ground-water recharge at soil saturation	m/s
paramNum	ct_index	Concentration time index (empirical Kirpich formula, for example)	s

Continued on next page

Table 3.2 – *Continued from previous page*

Type	Name	Description	Unit
paramNum	str_surf	Parameter to control retention of surface runoff	dimensionless
paramNum	str_pref	Parameter to control retention of preferential runoff	dimensionless
paramNum	str_inter	Parameter to control retention of medium-fast runoff	dimensionless
paramNum	str_base	Parameter to control retention in the ground-water reservoir	dimensionless
paramNum	relsat_etmin	Relative filling of soil reservoir below which evapotranspiration becomes zero	dimensionless (0...1)
paramNum	relsat_etmax	Relative filling of soil reservoir above which evapotranspitation is no longer moisture-limited	dimensionless (0...1)
paramNum	fac_precip	Precipitation correction factor (used for input updating, for example)	dimensionless
sharedParamNum	cropFac_slope	Constant "a" in "Makking crop factor = a * LAI + b"	dimensionless
sharedParamNum	cropFac_inter	Constant "b" in "Makking crop factor = a * LAI + b"	dimensionless
sharedParamNum	mult_surf	Factor applied to surface runoff before output (¡¿ 1 for tests only)	dimensionless
sharedParamNum	mult_pref	Factor applied to preferentialrunoff before output (¡¿ 1 for tests only)	dimensionless
sharedParamNum	mult_inter	Factor applied to medium-fast runoff before output (¡¿ 1 for tests only)	dimensionless
sharedParamNum	mult_base	Factor applied to slow runoff (base flow) before output (¡¿ 1 for tests only)	dimensionless
sharedParamNum	snow_a0	Constant describing the dependence of moisture and heat fluxes on wind speed (additive term in linear model)	m/s
sharedParamNum	snow_a1	Constant describing the dependence of moisture and heat fluxes on wind speed (factor in linear model)	dimensionless
sharedParamNum	snow_kSat	Saturated hydraulic conductivity of snow	m/s
sharedParamNum	snow_densDry	Density of dry snow	kg/m3
sharedParamNum	snow_specCapRet	Capillary retention volume as a fraction of the solid snow water equivalent	dimensionless
sharedParamNum	snow_emissivityMin	Minimum value of snow emissivity (for old snow surface)	dimensionless
sharedParamNum	snow_emissivityMax	Maximum value of snow emissivity (for old snow surface)	dimensionless
sharedParamNum	snow_tempAir_crit	Air temperature below which precipitation falls as snow	degree Celsius
sharedParamNum	snow_albedoMin	Minimum albedo of (old) snow	dimensionless
sharedParamNum	snow_albedoMax	Maximum albedo of (new) snow	dimensionless
sharedParamNum	snow_agingRate_tAirPos	Aging rate describing the decrease in snow albedo when air temperature is positive	1/s
sharedParamNum	snow_agingRate_tAirNeg	Aging rate describing the decrease in snow albedo when air temperature is negative	1/s
sharedParamNum	snow_soilDepth	Thickness of the soil column considered in computation of the snow energy balance	m
sharedParamNum	snow_soilDens	Density of the soil considered in computation of the snow energy balance	kg/m3
sharedParamNum	snow_soilSpecHeat	Specific heat capacity of the soil considered in computation of the snow energy balance	kJ/kg/K
sharedParamNum	snow_weightAirTemp	Weight used in the estimation of snow surface temperature from air temperature and mean snow temperature	dimensionless (0...1)
sharedParamNum	snow_fullShadowLAI	Reduces short-wave incoming radiation depeding on the LAI (rad'= rad * (1 - LAI/snow_fullShadowLAI))	m
sharedParamNum	heightZeroWind	Height above ground where wind speed approaches zero (used in precipitation correction)	m
output	qx_end	Outflow rate of the catchment at end of time step	m3/s
output	qx_avg	Outflow rate of the catchment, time step average	m3/s
output	swe	Snow water equivalent	m
output	etp	Rate of potential evapotranspiration	m/s

Continued on next page

Table 3.2 – *Continued from previous page*

Type	Name	Description	Unit
output	etr	Rate of actual evapotranspiration	m/s

3.2   Default reach class

3.2.1   Simulated processes

The reach class simulates the outflow from a river reach given information on the inflow and its storage character-
istics. The concept is described in Sec. 7.2.

3.2.2   Data members

A list of the data members of the class is provided in Table 3.3. See Kneis (2012b) for an explanation of the
abbreviations in the 'type' column.

Table 3.3: Data members of the default reach class.

Type	Name	Description	Unit
paramFun	v2k	Retention constant of the reach (s) as a function of storage (m3)	s
paramFun	q2k	Retention constant of the reach (s) as a function of flow rate (m3/s)	s
stateScal	vol	Storage volume of the reach	m3
inputSim	qi_end	Inflow rate at end of time step	m3/s
inputSim	qi_avg	Inflow rate, time step average	m3/s
output	qx_end	Outflow rate at end of time step	m3/s
output	qx_avg	Outflow rate, time step average	m3/s

3.3   Minireach class

3.3.1   Simulated processes

The minireach class simulates a reach (or pipe) of very short length so that the travel time is practically negligible.
Thus, the outflow a minireach object is identical to the inflow.

3.3.2   Data members

A list of the data members of the class is provided in Table 3.4. See Kneis (2012b) for an explanation of the
abbreviations in the 'type' column.

Table 3.4: Data members of the minireach class.

Type	Name	Description	Unit
inputSim	qi_end	Inflow rate at end of time step	m3/s
inputSim	qi_avg	Inflow rate, time step average	m3/s
output	qx_end	Outflow rate at end of time step	m3/s
output	qx_avg	Outflow rate, time step average	m3/s

3.4   Node classes

3.4.1   Simulated processes

The purpose of node objects is to merge flows from different sources. The typical case is a node with two inflows (e. g. a stream junction). Nodes with a higher numbner of inflows (or with just a single inflow) may be useful in some situations.

3.4.2   Data members

A list of the data members of the class is provided in Table 3.5 for the example of two inflows. See Kneis (2012b) for an explanation of the abbreviations in the 'type' column.

Table 3.5: Data members of the node class with two inflows.

Type	Name	Description	Unit
inputSim	qi_end_1	Inflow rate at end of time step (source 1)	m3/s
inputSim	qi_end_2	Inflow rate at end of time step (source 2)	m3/s
inputSim	qi_avg_1	Inflow rate, time step average (source 1)	m3/s
inputSim	qi_avg_2	Inflow rate, time step average (source 2)	m3/s
output	qx_end	Outflow rate at end of time step	m3/s
output	qx_avg	Outflow rate, time step average	m3/s

3.5   Lake class

3.5.1   Simulated processes

The class simulates the outflow from an uncontrolled lake/reservoir based on a rating curve and a storage curve. Precipitation and evaporation losses are taken into account. Details are described in Sec. 10.2.

3.5.2   Data members

A list of the data members of the class is provided in Table 3.6. See Kneis (2012b) for an explanation of the abbreviations in the 'type' column.

Table 3.6: Data members of the lake class.

Type	Name	Description	Unit
stateScal	v	Storage volume	m3
stateScal	vp	Total precipitation input within a time step (temporary variable to compute the mass balance)	m3
stateScal	ve	Total evaporation loss within a time step (temporary variable to compute the mass balance)	m3
inputSim	qi_end	Inflow rate at end of time step	m3/s
inputSim	qi_avg	Inflow rate, time step average	m3/s
paramNum	area_max	Maximum water surface area (area collecting precipitation)	m2
paramNum	fac_precip	Precipitation correction factor (used for input updating, for example)	dimensionless
paramFun	v2h	Storage curve (water level as a function of the storage volume)	m

<p style="text-align:center">Table 3.6 – *Continued from previous page*</p>

Type	Name	Description	Unit
paramFun	h2q	Rating curve at the lake's outflow (outflow rate as a function of the water level)	m3/s
paramFun	h2a	Function to compute the evaporating surface area from the water level	m2
inputExt	precip	Precipitation (time series)	mm / time step
inputExt	glorad	Short-wave radiation (time series)	W/m2
inputExt	tavg	Average air temperature (time series)	degree Celsius
output	qx_end	Outflow rate at end of time step	m3/s
output	qx_avg	Outflow rate, time step average	m3/s
output	h	Water level	m

3.6   Gage class

3.6.1   Simulated processes

In many situations it is sufficient to output the simulated flow rate of a river reach, making the explicit simulation of a gage object unnecessary. The advantage of instantiating an object of the gage class lies in the fact that the simulated flow may be optionally substituted by observed values. This is quite useful, for example, when a calibrating a model for the part of a river basins located downstream of a gage.

3.6.2   Data members

A list of the data members of the class is provided in Table 3.7. See Kneis (2012b) for an explanation of the abbreviations in the 'type' column.

Table 3.7: *Data members of the gage class.*

Type	Name	Description	Unit
inputSim	qi_end	Simlulated inflow rate at end of time step	m3/s
inputSim	qi_avg	Simulated inflow rate, time step average	m3/s
inputExt	qobs_avg	Observed flow, time step average. May be used as an optional substitute for the simulated inflow.	m3/s
paramNum	obs_lbound	Threshold; The sim. flow (qi) is substituted by the obs. flow (qobs) only if qobs is greater/equal obs_lbound	m3/s
paramNum	obs_ubound	Threshold; The sim. flow (qi) is substituted by the obs. flow (qobs) only if qobs less/equal obs_ubound	m3/s
output	qx_end	Outflow rate at end of time step	m3/s
output	qx_avg	Outflow rate, time step average	m3/s

3.7   Rain gage class

3.7.1   Simulated processes

Objects of this class can be used to query the precipitation at a point as computed from residual interpolation.

3.7.2   Data members

A list of the data members of the class is provided in Table 3.8. See Kneis (2012b) for an explanation of the abbreviations in the 'type' column.

Table 3.8: *Data members of the rain gage class.*

Type	Name	Description	Unit
inputExt	precip_resid	Residuals of precipitation (time series)	mm / time step
inputExt	precip_slope	Slope of the linear model precip ~ elevation	mm / time step / meter
inputExt	precip_inter	Intercept of the linear model precip ~ elevation	mm / time step
paramNum	elev	Elevation	m
output	precip	Precipitation	mm / time step

3.8   External inflow class

3.8.1   Simulated processes

This class provides a simple means to represent an external water source. The time-variable flow rates are pre-defined, i. e. read from a file. The class may also be helpful if a large-scale model is split into sub-models at the boundaries of major watersheds. In such a case, it may be desireable to save the runoff from an upstream area (sub-model A) to a file and re-read the data later when simulating the downstream part (sub-model B).

3.8.2   Data members

A list of the data members of the class is provided in Table 3.9. See Kneis (2012b) for an explanation of the abbreviations in the 'type' column.

Table 3.9: *Data members of the external inflow class.*

Type	Name	Description	Unit
inputExt	precip_resid	Residuals of precipitation (time series)	mm / time step
inputExt	precip_slope	Slope of the linear model precip ~ elevation	mm / time step / meter
inputExt	precip_inter	Intercept of the linear model precip ~ elevation	mm / time step
paramNum	elev	Elevation	m
output	precip	Precipitation	mm / time step

3.8.3   Reservoir class

This class is still experimental and not documented.

3.8.4   Flood control storage basin class

This class is still experimental and not documented.

Part III

Mathematical description of hydrological processes

Chapter 4

Dynamics of the snow cover

4.1 Energy balance method

4.1.1 Capabilities and limitations

In many catchments, snow storage and melting are important components of the water cycle. Snow melt, possibly accompanied (or caused) by rainfall is a major cause of flood generation in many catchments. However, the structure of a natural snow cover is very complex and the simulation of its dynamics is difficult. Therefore, any snow model is subject to a number of simplyfing assumptions and limitations. The most important limitations of the snow model described in this section are:

- The snow pack is treated as homogeneous (well mixed) layer. Thus, possible stratification is neglected.

- Shortwave radiation is not corrected for slope and aspect, i. e. the model should be applied only to horizontal surfaces or larger areas where the effects of slope and aspect may be assumed to level out.

- The current model does not account for vegetation cover. In reality, vegetation may affect the snow dynamics in many ways (e. g. due to interception, sheltering, shadowing, long-wave emission, etc.).

4.1.2 Basics of the energy balance method

4.1.2.1 State variables

A physically-based simulation of the snow dynamics requires the water equivalent and the energy content of the snow pack to be considered as state variables (e. g. Dyck and Peschke, 1995; Tarboton and Luce, 1996). In

the model described here, the snow albedo is introduced as an auxiliary state variable.

Snow water equivalent   The snow water equivalent, SWE (m), represents the total volume of water (stored in solid and liquid form) contained in a snow pack covering an area of 1 m^2. SWE is defined by Eqn. 4.1

$$\Psi SWE = SH \cdot \frac{\rho_{snow}}{\rho_w} \qquad (4.1)$$

where SH is the snow height (m) and ρ_{snow} and ρ_w represent the densities of snow and water (kg/m^3). The unit of SWE or the snow height (meters) is equivalent to m^3/m^2. To convert from units of m to units of kg/m^2, one has to multiply SWE with the density of *water* ρ_w in kg/m^3 (even though a part or all of the stored water is in solid form).

Energy content   The energy content, SEC (kJ/m^2), represents the energy stored in the snow pack. SEC is defined relative to a reference energy content ($SEC= 0$ for ice at 0°C) as detailed below.

Snow albedo   The snow albedo AS (–) represents the reflectivity of the snow surface for shortwave radiation. At each snowfall event, the snow surface is re-born and the albedo is reset to its maximum value associated with freshly fallen snow.

4.1.2.2 Processes

The dynamics of SWE is described by the mass balance and the dynamics of SEC is controlled by the energy balance. Both mass and energy balance are coupled as illustrated in Fig. 4.1. A simulation of the state variables therefore requires a simultaneous solution of

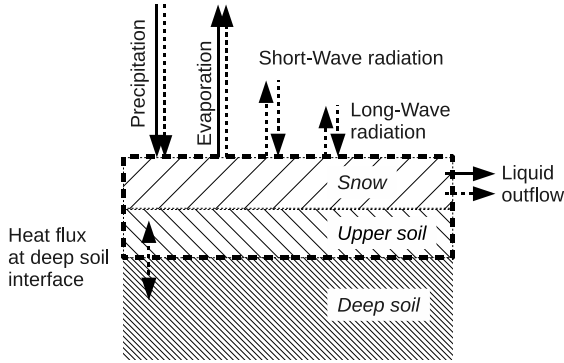differential equations summarized in Table 4.1 using a matrix notation.

Figure 4.1: *Fluxes of mass (solid arrows) and heat (dashed arrows) to be considered when simulating the snow dynamics.*

4.1.2.3   Definition of the energy content

The energy content of the snow cover, SEC, can only be defined with respect to some reference. A useful reference state is ice at a temperature of $0°$C for which SEC is zero by convention (Tarboton and Luce, 1996). With that reference, the relation between the energy content SEC and the (average) snow temperature T_s follows from the considerations below:

1. Negative values of SEC indicate that SWE consists of solid water only and the snow temperature is negative. The relation between temperature and energy content is then determined by the heat capacity of the ice mass according to Eqn. 4.2 (see Table 4.2 for definition of symbols).

$$\frac{dT_s}{dSEC} = \frac{1}{SWE \cdot \rho_w \cdot C_{ice}} \tag{4.2}$$

With respect to the energy content, it is useful to treat the snow cover and the upper soil up to a certain depth D_s as a single system (dashed box in Fig. 4.1). The upper soil is defined as the layer which thermally interacts with the snow cover on short time scales. Then, Eqn. 4.2 expands to Eqn. 4.3, where D_s (m) represents the depth of the upper soil, ρ_s (kg/m^3) is the soil density and C_s (kJ/kg/K) is the soil's specific heat capacity.

$$\frac{dT_s}{dSEC} = \frac{1}{SWE \cdot \rho_w \cdot C_{ice} + D_s \cdot \rho_s \cdot C_s} \tag{4.3}$$

Then advantage of treating the snow cover and the upper soil as a single system is that the soil energy flux reduces to the long-term average flux at the interface between shallow and deep soil (see Fig. 4.1). This flux is much less variable and may be approxiamed by a constant.

2. If SEC is zero, the temperature is $0°$C and the snow cover still does not contain liquid water as a consequence of the chosen reference.

3. At positive values of SEC, some fraction of SWE exists in liquid form. As long as ice and liquid water coexist, the snow temperature remains at $0°$C and all energy input is consumed by the melting process. The energy required to completely melt a snow cover at a temperature of $0°$C which consists of solid water only is determined by the ice's heat of fusion (see Table 4.2) and equals (Eqn. 4.4):

$$SWE \cdot \rho_w \cdot H_{ice} \tag{4.4}$$

4. There is a critical value of SEC where all ice was melted and only liquid water is left. The snow has ceased to exist. If more energy is input, the temperature of the liquid water rises above zero according to Eqn. 4.5 (see Table 4.2 for definition of symbols).

$$\frac{dT_s}{dSEC} = \frac{1}{SWE \cdot \rho_w \cdot C_{wat}} \tag{4.5}$$

Based on these considerations, the relation between SEC and T_s can be computed for a snow cover with a given SWE as illustrated in Fig. 4.2.

With the basic relations given by Eqn. 4.2–4.5 we can infer from the energy content SEC two important variables: the temperature T_s of the snow pack and the dimensionless fraction of liquid water SLF.

4.1.2.4   Snow temperature

As the snow temperature is not simulated explicitly, it needs to be inferred from the state variables. Since snow is a good isolator, the snow surface temperature, T_{ss}, is generally different from the depth-averaged snow temperature T_s (Tarboton and Luce, 1996).

Table 4.1: *Process matrix of the energy balance snow model describing the dynamics of the state variables. The rate expressions containing state variables, forcings, and parameters are derived in Sec. 4.1.4 & 4.1.5. The stoichiometry factors f_{prec}, f_{subl}, and f_{flow} (kJ/m³) used to convert between mass and energy are derived in Sec. 4.1.2.6. The (+) indicates that precipitation has an impact on the albedo but this is considered a separate process called 'Albedo evolution' (see Sec. 4.1.3).*

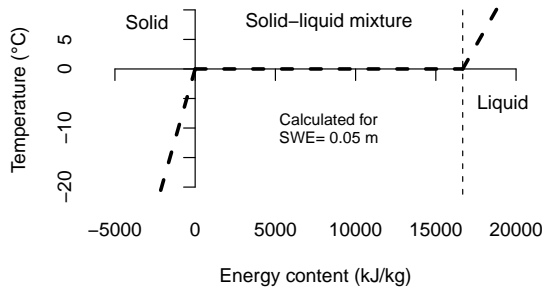| Process	Stoichiometry factors			Rate expr.	Rate units
	SEC (kJ/m²)	SWE (m)	AS (−)		
Short-wave radiation balance	0.001	0	0	R_{netS}	W/m²
Long-wave radiation balance	0.001	0	0	R_{netL}	W/m²
Soil heat flux	0.001	0	0	R_{soil}	W/m²
Sensible heat flux	0.001	0	0	R_{sens}	W/m²
Precipitation	f_{prec}	1	(+)	M_{prec}	m/s
Sublimation	$-f_{subl}$	−1	0	M_{subl}	m/s
Melt water outflow	$-f_{flow}$	−1	0	M_{flow}	m/s
Albedo evolution	0	0	1	G_{alb}	1/s

Figure 4.2: *Relation between energy content and temperature for a sample snow cover with SWE= 0.05 m (soil interaction not taken into account). The thin vertical dashed line marks the (theoretical) energy content when the snow cover consists of liquid water only, i. e. when all ice was melted.*

Depth-averaged temperature   Since the snow pack is assumed to be homogeneous, only the depth-averaged value, T_s, is directly accessible through the state variables SEC and SWE. Three cases need to be distinguished (see Sec. 4.1.2.3 for definition of D_s, ρ_s and C_s):

Case 1: $(SEC < 0)$

$$T_s = \frac{SEC}{SWE \cdot \rho_w \cdot C_{ice} + D_s \cdot \rho_s \cdot C_s} \qquad (4.6)$$

Case 2: $(0 < SEC < SWE \cdot \rho_w \cdot H_{ice})$

$$T_s = 0 \qquad (4.7)$$

Table 4.2: *Snow-related physical constants (Tarboton and Luce, 1996; Dyck and Peschke, 1995).*

Symbol	Value	Unit	Description
ρ_i	≈922	kg/m³	Density of ice
C_{ice}	2.09	kJ/kg/K	Specific heat of ice
H_{ice}	333.5	kJ/kg	Latent heat of ice fusion (melt heat)
E_{ice}	2837	kJ/kg	Latent heat of ice sublimation ($=H_{ice}+E_{wat,0}$)
ρ_w	1000	kg/m³	Density of water
C_{wat}	4.18	kJ/kg/K	Specific heat of water
$E_{wat,0}$	2503	kJ/kg	Latent heat of water evaporation at 0°C

Case 3: $(SEC > SWE \cdot \rho_w \cdot H_{ice})$

$$T_s = \frac{SEC - SWE \cdot \rho_w \cdot H_{ice}}{SWE \cdot \rho_w \cdot C_{wat} + D_s \cdot \rho_s \cdot C_s} \qquad (4.8)$$

The equation for the first case (Eqn. 4.6) directly follows from Eqn. 4.3 by multiplying with a negative ΔSEC. The resulting temperature T_s is negative.

The conditions when Eqn. 4.7 must be used (second case) follow from the definition of SEC and Eqn. 4.4.

The third case (Eqn. 4.8) is considered here only for completeness since in represents the case where all snow became liquid, and T_s actually represents a water temperature.

Surface temperature To compute energy fluxes across the snow-atmosphere interface (outgoing long wave radiation, exchange of sensible heat, etc.), an estimate of the surface temperature T_{ss} is required.

For estimating T_{ss}, Tarboton and Luce (1996) assume that the energy fluxes at the snow surface are in equilibrium. T_{ss}, which controls some of the flux rates, is determined iteratively as the surface temperature where all energy fluxes balance. They also introduce a tuning parameter (snow surface conductance).

To avoid iteration, the very simple approach presented in Eqn. 4.9 is used here to estimate T_{ss}. Therein, TA (°C) is the air temperature and μ is a weighting parameter. If $\mu = 0$, the surface temperature T_{ss} is taken to be equal to the depth-averaged temperature T_s and if $\mu = 0.5$, the surface temperature is simply computed as the mean of T_s and TA. Eqn. 4.9 accounts for the fact that T_{ss} cannot become greater than 0 °C.

$$T_{ss} = \begin{cases} 0 & \text{if } T_s = 0 \\ min(0, (1 - \mu) \cdot T_s + \mu \cdot TA) & \text{if } T_s < 0 \end{cases}$$

(4.9)

4.1.2.5   Fraction of liquid water

In a melting snow cover, solid and liquid water coexist. To estimate the actual rate of water outflow, the fraction of liquid water, SLF (–), must be known. Since SLF is not simulated explicitly, it needs to be inferred from state variables. Taking into account that $SLF=0$ if $SEC=0$ by definition and that the energy required to completely melt all ice ($SLF=1$) is given by Eqn. 4.4, the liquid fraction can be computed from the energy content SEC as (Eqn. 4.10)

$$SLF = \frac{SEC}{SWE \cdot \rho_w \cdot H_{ice}}$$

(4.10)

for $0 \leq SEC \leq SWE \cdot \rho_w \cdot H_{ice}$, i. e. for snow at 0 °C. Thus, in practice one should use something like $min(1, max(0, SLF))$ if the condition is not checked explicitly. Note that SLF represents a *mass fraction* (Tarboton and Luce, 1996), not a volume fraction. Thus, SLF can also be written as in Eqn. 4.11,

where m_w and m_i represent the masses of water and ice per m² respectively.

$$SLF = \frac{m_w}{m_w + m_i}$$

(4.11)

Eqn. 4.11 may be transformed into Eqn. 4.10 as follows:

Numerator: As we are dealing with melting snow, the water mass m_w is at 0 °C. Due to the definition of the energy content (see Sec. 4.1.2.3), the mass m_w (kg/m²) can be substituted by SEC/H_{ice}. SEC (kJ/m²) represents the energy content associated with m_w and H_{ice} is the fusion heat of ice (kJ/kg).

Denominator: The sum $m_w + m_i$ in the denominator of Eqn. 4.11 represents the snow mass per square meter, m_s (kg/m²). If m_s is written as the product of snow density ρ_{snow} (kg/m³) and snow height SH (= snow volume per m² in meters), it follows from Eqn. 4.1 that the denominator $m_w + m_i$ equals $SWE \cdot \rho_w$.

4.1.2.6   Relations between mass and energy fluxes

In this section, the conversion factors f_{prec}, f_{subl}, and f_{flow} (kJ/m³) appearing in Table 4.1 are derived. The values of the involved physical constants can be found in Table 4.2.

Precipitation The energy flux (kJ/m²/s) resulting from precipitation input is obtained by multiplying the mass flux (m/s) with f_{prec} (kJ/m³). For liquid precipitation, f_{prec} is given by Eqn. 4.12 and Eqn. 4.13 applies to solid precipitation (snowfall). Note that precipitation is a water equivalent, thus, the density of water (not the one of ice) must be used when converting from depth (m) to mass (such as kg/m²).

Case 1: $(TA > T_{crit})$

$$f_{prec} = \rho_w \cdot C_{wat} \cdot max(TA, 0) + \rho_w \cdot H_{ice} \quad (4.12)$$

Case 2: $(TA <= T_{crit})$

$$f_{prec} = \rho_w \cdot C_{ice} \cdot min(TA, 0)$$

(4.13)

In Eqn. 4.12 and 4.13, TA (°C) is the air temperature and T_{crit} (°C) is the threshold temperature for rain/snow fall. An approach for mixed precipitation is presented in Tarboton and Luce (1996). The value of f_{prec} computed with Eqn. 4.12 is always positive and it is always negative if Eqn. 4.13 is ised. Note that the second

term in Eqn. 4.12 accounts for the fact that the water is liquid and therefore has a positive energy content even at 0°C (see definition of SEC in Sec. 4.1.2.3).

Sublimation The energy flux due to sublimation (kJ/m^2/s) is obtained by multiplying the corresponding mass flux (m/s) with f_{subl} (kJ/m^3) defined in Eqn. 4.14. The constant E_{ice} integrates the latent heat of both melting and evaporation (see Table 4.2). As heat is lost from the snow pack, the energy flux has a negative sign in Table 4.1.

$$f_{subl} = \rho_w \cdot E_{ice} \qquad (4.14)$$

Meltwater outflow To obtain the energy flux (kJ/m^2/s) corresponding to the outflow of water from the snow pack (m/s) one has to multiply the latter by f_{flow} (kJ/m^3) defined in Eqn. 4.15. The expression reflects that the energy of water at 0°C equals H_{ice} as a consequence of the chosen reference for SEC (see Sec. 4.1.2.3). As heat is lost from the snow pack, the energy flux has a negative sign in Table 4.1.

$$f_{flow} = \rho_w \cdot H_{ice} \qquad (4.15)$$

4.1.3   Simulation of the snow albedo

There are many approaches to estimate the snow albedo AS (–) with different level of sophistication. In general, the albedo is an average value accounting for the reflection of both visible and near infrared solar radiation. After snowfall, AS generally decreases due to various processes such as metamorphosis and pollution of the snow surface. Here, a very simple aging approach cited by Dyck and Peschke (1995) was adopted. The original equation to describe the dependence of AS on the age of the snow surface (Equation 10.40 in Dyck and Peschke, 1995) is a power function (Eqn. 4.16) where AS_{min} is the minimum value that AS approaches after a long time without snowfall and AS_{rng} is the difference between the maximum AS right after snowfall and AS_{min}. Furthermore, Δt is the age of the snow surface and k (1/time) is a rate constant to describe the intensity of the aging process.

For convenience, Eqn. 4.16 was rewritten in an exponential form (Eqn. 4.17) and AS_{rng} was expanded to $(AS_{max} - AS_{min})$. In the final rearrangement, the new parameter k_{AS} was introduced which is related to the parameter k of the original power equation (Eqn. 4.16)

by $k_{AS} = -k \cdot ln(AS_{max} - AS_{min})$. Note that reasonable values of AS are < 1 why $ln(AS_{max} - AS_{min})$ is always negative and the minus sign is required to define k_{AS} as a positive constant.

$$
\begin{aligned}
AS &= AS_{min} + AS_{rng}{}^{(1+\Delta t \cdot k)} && (4.16)\\
&= AS_{min} + AS_{rng} \cdot AS_{rng}{}^{\Delta t \cdot k}\\
&= AS_{min} + AS_{rng} \cdot exp(ln(AS_{rng}{}^{\Delta t \cdot k}))\\
&= AS_{min} + AS_{rng} \cdot exp(\Delta t \cdot k \cdot ln(AS_{rng}))\\
&= AS_{min} + (AS_{max} - AS_{min}) \cdot e^{-k_{AS} \cdot \Delta t}
\end{aligned}
$$
$$(4.17)$$

The advantage of Eqn. 4.17 over the original power function (Eqn. 4.16) is the much simpler derivative with respect to time which is given in Eqn. 4.18. Note that the definition of AS (Eqn. 4.17) was used to simplify the derivative and that, in this way, the surfage age (Δt) was eliminated from the expression.

$$
\begin{aligned}
\frac{dAS}{dt} &= (AS_{max} - AS_{min}) \cdot e^{-k_{AS} \cdot \Delta t} \cdot (-k_{AS})\\
&= (AS - AS_{min}) \cdot (-k_{AS}) && (4.18)
\end{aligned}
$$

Considering that the snow surface is renewed when new snow falls, the process rate G_{alb} (1/s) controlling the albedo (see Table 4.1) may be expressed by Eqn. 4.19.

$$
G_{alb} = \begin{cases} (AS_{max} - AS) & \text{if snowing} \\ k_{AS}(TA) \cdot (AS_{min} - AS) & \text{else} \end{cases}
$$
$$(4.19)$$

where $X = 1$ if $((PI \dot{\iota} \ 0) \ \& \ (TA \dot{\iota} \ T_{crit}))$ and $X = 0$ otherwise. Note that the applied value of the rate constant k_{AS} depends on wether the air temperature is above or below 0 °C (Dyck and Peschke, 1995) . Thus, G_{alb} is affected by both the precipitation intensity PI and air temperature TA. In the current model version, the albedo is independend of the snow height, i. e. there is no reduction when the snow cover becomes shallow.

Recommended values of the parameters are given in Table 4.3. A synthetic example illustrating the dynamics of the albedo in response to precipitation and temperature is shown in Fig. 4.3.

Table 4.3: *Parameters controlling the snow albedo based on* Dyck and Peschke *(1995). With respect to k_{AS}, the factor 1/86400 converts from 1/d to 1/s and the term $ln(AS_{max} - AS_{min})$ accounts for the structural difference between Eqn. 4.17 and Eqn. 4.16.*

Symbol	Units	Value
AS_{min}	–	0.35–0.4
AS_{max}	–	0.75–0.9
$k_{AS}(TA \geq 0)$	1/s	$-0.12/86400$ $\cdot$
		$ln(AS_{max} - AS_{min})$
$k_{AS}(TA < 0)$	1/s	$-0.05/86400$ $\cdot$
		$ln(AS_{max} - AS_{min})$

4.1.4 Energy flux rates

4.1.4.1 Short-wave radiation balance

The short-wave net radiation (or short-wave radiation balance), R_{netS} (W/m^2) is computed from Eqn. 4.20

$$R_{netS} = SR \cdot (1 - AS) \tag{4.20}$$

where SR is the incoming solar (i. e. short-wave) radiation (W/m^2) and AS (–) is the corresponding albedo of the snow surface (see Sec. 4.1.3). If measured values of SR are unavailable, they can be estimated as described in Tarboton and Luce (1996) or Dyck and Peschke (1995). No corrections for slope and aspect are made here as it is assumed that the effects level out for larger areas. If the model is applied locally, slope and aspect might need to be taken into account by reducing/amplifying the measured (or computed) solar radiation for a horizontal surface.

The presence of a dense vegetation cover (coniferous forest) may considerably reduce the amount of incoming short-wave radiation. An ad-hoc approach to estimate the corrected incoming short-wave radiation SR' due to shadowing is presented in Eqn. 4.21

$$SR' = SR \cdot (1 - \frac{LAI}{LAI_{r0}}) \tag{4.21}$$

where LAI is the leaf-area index (m^2/m^2) and LAI_{r0} is an empirical parameter. Conceptually, LAI_{r0} represents the leaf-area index where short-wave radiation is extincted completely. According to Ludwig and Bremicker (2006), a reduction of incoming short-wave by 30% can be assumed for coniferous forest. Assuming a leaf-area index for coniferous forest of 11
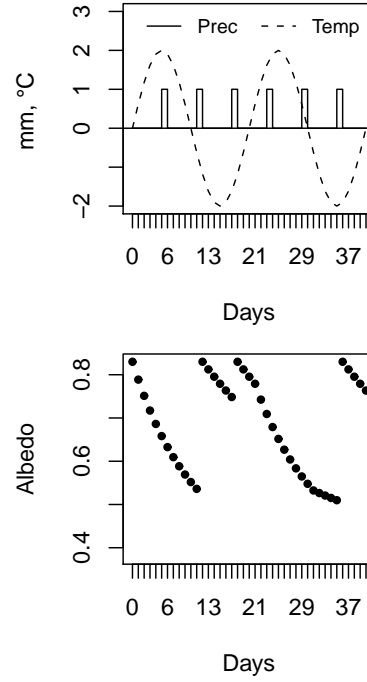

Figure 4.3: *Synthetic example illustrating the dynamics of the albedo as affected by temperature and precipitation. Snowfall was assumed at temperatures below 0 °C. For AS_{min} and AS_{max}, the means of the ranges given in Table 4.3 were used.*

(Ludwig and Bremicker, 2006, page 11), this results in $LAI_{r0} \approx 36$.

4.1.4.2 Long-wave radiation balance

The long-wave radation balance R_{netL} (W/m^2) is the difference between the incoming long-wave radiation emitted from clear sky and clouds, R_{inL}, and the long-wave emission of the snow pack, R_{outL} (Eqn. 4.22).

$$R_{netL} = R_{inL} - R_{outL} \tag{4.22}$$

According to the Stefan-Boltzmann equation (Eqn. 4.23), emissions R are proportional to the fourth power of temperature T (here in °C), with σ being the Stefan-Boltzmann constant (=5.67e-08 W/m^2/K^4) and ε being the dimensionless emissivity (range 0–1 with 1 for a black body).

$$R = \varepsilon \cdot \sigma \cdot (T + 273.15)^4 \tag{4.23}$$

Outgoing part   The emission of the snow pack, R_{outL} (W/m^2), can directly be computed from Eqn. 4.23 substituting T by the snow surface temperature T_{ss} (see Eqn. 4.9). The emissivity of snow is about ε=0.82 for old snow and ε=0.99 for fresh snow (Dyck and Peschke, 1995). A pragmatic way to account for the age of the snow pack is to relate ε to the dynamically computed albedo AS (see Sec. 4.1.3) as in Eqn. 4.24.

$$\varepsilon = \varepsilon_{min} + (\varepsilon_{max} - \varepsilon_{min}) \cdot \frac{AS - AS_{min}}{AS_{max} - AS_{min}} \quad (4.24)$$

Incoming part   Note: The following section is based on the German wikipedia site for the term 'Atmosphärische Gegenstrahlung' as this was the most transparent and concise source of information.

The incoming long-wave R_{inL} is harder to estimate. Generally, it is distinguished between clear-sky emissions ($R_{inL,cs}$) and emissions by clouds ($R_{inL,cl}$). A transparent formulation is given by Eqn. 4.25 where $R_{inL,cs}$ and $R_{inL,cl}$ are estimated individually and FC represents the degree of cloud cover (range 0–1). It is (legitimately) assumed that long-wave emissions mainly stem from the lower atmshpere (whose state is approximately known from ground measurements).

$$R_{inL} = (1 - FC) \cdot R_{inL,cs} + FC \cdot R_{inL,cl} \quad (4.25)$$

For the cloud cover FC (–), measured values must be used or FC needs to be estimated from a comparison of actual solar radiation to the theoretical maximum value depending on the day of the year and the latitude. However, the latter approach can only yield daily estimates of FC as it does not work during nighttime.

Incoming part (Clear sky emissions)   The clear sky radiation $R_{inL,cs}$ appearing in Eqn. 4.25 is computed from the Stefan-Bolzmann equation (Eqn. 4.23) substituting T by the air temperature TA and using a value of the emissivity ε representative for a clear sky. Hock (2005) lists various empirical formulas for estimation of the clear-sky ε based on athmospheric temperature and/or vapor pressure. Some formulas are compared in Fig. 4.4.

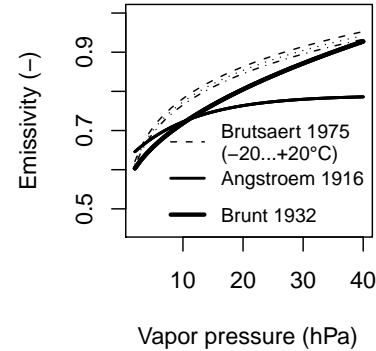Here, we selected the simple formula developed by Brunt (Eqn. 4.26) which estimates the clear-sky ε as a

Figure 4.4: *Comparison of different empirical formulas for clear sky emissivity.*

function of the vapor pressure e in hPa (see Hock, 2005, p.373).

$$\varepsilon = 0.51 + 0.066 \cdot \sqrt{e} \quad (4.26)$$

Incoming part (Cloud emissions)   Finally, the long-wave emissions of the clouds ($R_{inL,cl}$ in Eqn. 4.25) are also computed using Eqn. 4.23. The clouds are treated as a black body, thus ε is set to 1. A reasonable estimate of the clouds' bottom-side temperature is the dew point temperature T_{dew} (°C). T_{dew} represents the temperature to which a parcel of air with a specific content of vapor must be cooled, for water vapor to condense. Thus, T_{dew} is the temperature at which air with a specific vapor content becomes saturated. T_{dew} can be computed by rearranging the Magnus-Equation (Eqn. 4.35) for the temperature T (Eqn. 4.27). The reagrranged Eqn. 4.35 yields the temperature at which, for a given vapor pressure, saturation would occur. Thus, the actual vapor pressure e (not E) must be inserted in the rearranged Eqn. 4.35. If, as usual, only relative humidity and temperature are given, the value of e must be obtained from Eqn. 4.34 with E beign computed with Eqn. 4.35 (now without rearrangement).

Thus, the dewpoint temperature T_{dew} follows from Eqn. 4.27 with e being computed from RH (%) and TA

(°C) after Eqn. 4.35. Results for a range of temperatures and relative humidities are presented in Fig. 4.5.

$$T_{dew} = \begin{cases} \dfrac{237.3 \cdot log_{10}(e/6.11)}{7.5 - log_{10}(e/6.11)} & \text{over water} \\[2ex] \dfrac{265.5 \cdot log_{10}(e/6.11)}{9.5 - log_{10}(e/6.11)} & \text{over ice} \end{cases} \quad (4.27)$$
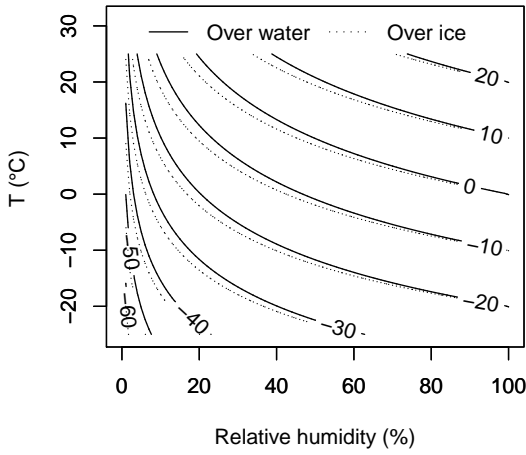

Figure 4.5: *Dewpoint temperature as a function of temperature and relative humidity as computed with Eqn. 4.27.*

4.1.4.3   Soil heat flux

The soil heat flux R_{soil} (W/m^2) is, in this model, the long-term average flux at the interface between upper and deep soil (recall Sec. 4.1.2.3). R_{soil} is taken as zero if not known (Tarboton and Luce, 1996).

4.1.4.4   Sensible heat flux

The flux of sensible heat, R_{sens} (W/m^2), is assumed to be proportional to the gradient of temperature between atmosphere (TA) and snow surface (T_{ss}, see Eqn. 4.9) as expressed by Eqn. 4.28. In this equation, D is a turbulent transfer coefficient (m/s), and ρ_a (kg/m^3) and C_{air} (kJ/kg/K) represent the density and the specific heat capacity of air, respectively. This expression is

equivalent to Equation 34 in Tarboton and Luce (1996) or Equation 10.43 in Dyck and Peschke (1995).

$$R_{sens} = D \cdot \rho_a \cdot C_{air} \cdot 10^3 \cdot (TA - T_{ss}) \quad (4.28)$$

The value of the air specific heat capacity is C_{air}= 1.005 kJ/kg/K (Tarboton and Luce, 1996). The density of air ρ_a (kg/m^3) is estimated from Eqn. 4.29 (see Equation 4.9 in Dyck and Peschke, 1995) that represents the ideal gas law (PA: air pressure in hPa, TA: air temperature in °C, specific gas constant for dry air: 0.287 kJ/kg/K, base of the Celsius-scale: 273.15 K).

$$\rho_a = \frac{PA \cdot 0.1}{0.287 \cdot (273.15 + TA)} \quad (4.29)$$

The values of C_{air} and ρ_a relate to dry air. However, the error in pressure due to neglection of moisture is rather low. Even at saturation, the vapor pressure is in the order of 0.5–2.5 % of the air pressure only for temperatures between 0–25 °C (see Fig. 4.6). The error in the estimate of the specific heat capacity is small as well. The value is about 1.005 kJ/kg/K for dry air (Tarboton and Luce, 1996) and about 1.013 kJ/kg/K for moist air (Dyck and Peschke, 1995, page 188, Eqn. 11.15)

The turbulent transfer coefficient D (m/s) in Eqn. 4.28 is a calibration parameter. Several approaches to estimate D do exist (e. g. Dyck and Peschke, 1995; Tarboton and Luce, 1996) making assumptions on the stability of the atmosphere and introducing other unknown parameters. Here, as in Knauf (1980), a simple approach is used that assumes a linear dependence of D on the wind speed WS in m/s according to Eqn. 4.30. The empirical coefficients a_0 and a_1 are dimensionless and must be determined by calibration.

$$D = a_0 + a_1 \cdot WS \quad (4.30)$$

4.1.5   Mass flux rates

4.1.5.1   Precipitation

The mass flux due to precipitation, M_{prec} (m/s), is computed from the precipitation intensity in units of mm/Δt by Eqn. 4.31 where Δt is the length of the time step in seconds (e. g. Δt=3600 for hourly precipitation data).

$$M_{prec} = \frac{PI}{10^3 \cdot \Delta t} \quad (4.31)$$

The corresponding energy fluxes are given by Eqn. 4.12 & 4.13, respectively.

4.1.5.2   Sublimation

The mass flux due to sublimation, M_{subl} (m/s) is proportional to gradient of vapor pressure between the air and the snow surface as expressed by Eqn. 4.32. In this expression, D is a turbulent transfer coefficient (m/s), ρ_a and ρ_w (kg/m^3) represent the densities of air and water. The symbols q and q_s denote the specific humidities (–) above and at the snow surface, respectively. This expression is equivalent to Equation 35 in Tarboton and Luce (1996) or Equation 10.44 in Dyck and Peschke (1995) (with changed sign) after multiplication with the density of water ρ_w to obtain the mass flux in kg/m^2/s.

$$M_{subl} = D \cdot \frac{\rho_a}{\rho_w} \cdot (q_s - q) \qquad (4.32)$$

Only positive values of M_{subl} are considered. The density of (dry) air ρ_a is estimated from Eqn. 4.29 (Sec. 4.1.4.4). The specific humidity (–) can be computed from vapor pressure e and air pressure PA (both in hPa) according to Eqn. 4.33 (see Equation 4.10 in Dyck and Peschke, 1995).

$$q = \frac{0.622 \cdot e}{PA - 0.378 \cdot e} \qquad (4.33)$$

Note that a commonly used approximation of Eqn. 4.33 is $q \approx 0.622 \cdot e/PA$ (Dyck and Peschke, 1995). This approximation is used, for example, by Tarboton and Luce (1996) in the derivation of their Equation 42. Note that they also substitute the pressure PA by the product of temperature, air density, and the dry air gas constant according to the ideal gas law.

The vapor pressure e (hPa) is derived from the relative humidity RH (%) by Eqn. 4.34 taking into account the vapor pressure at saturation E which is a function of temperature T.

$$e = \frac{RH}{100} \cdot E(T) \qquad (4.34)$$

E is commonly estimated with the Magnus equation (Eqn. 4.35, Fig. 4.6) given by Dyck and Peschke (1995). The temperature T is the air temperature in °C.

$$E(T) = \begin{cases} 6.11 \cdot 10^{\frac{7.5 \cdot T}{237.3+T}} & \text{over water} \\ 6.11 \cdot 10^{\frac{9.5 \cdot T}{265.5+T}} & \text{over ice} \end{cases} \qquad (4.35)$$
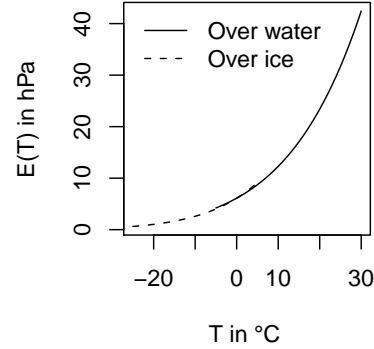

Figure 4.6: *Saturation vapor pressure over water and ice as a function of temperature (Magnus formula, Eqn. 4.35).*

When computing the input values for Eqn. 4.32, the saturation vapor pressure over ice (2nd form of Eqn. 4.35) must be used. When calculating the specific humidity of the atmosphere (q), one uses measured values of the air temperature, relative humidity, and air pressure in Eqn. 4.33 & 4.34. When computing the specific humidity at the snow surface (q_s), it is commonly assumed that the air is saturated at the surface temperature (Tarboton and Luce, 1996). Thus, one has to use $RH = 100$ and $T = T_{ss}$ in Eqn. 4.34 (see Eqn. 4.9 for the surface temperature T_{ss}).

For the turbulent transfer coefficient D (m/s), the same value is assumed as for the transfer coefficient of sensible heat (see Eqn. 4.30 in Sec. 4.1.4.4).

4.1.5.3   Melt water outflow

The mass flux due to meltwater outflow, M_{flow} (m/s) equals the snow pack's actual hydraulic conductivity (Male and Gray, 1981, cited in Tarboton and Luce (1996)). The actual hydraulic conductivity depends on both the saturated hydraulic conductivity $k_{sat,snow}$ (m/s) and the availablability of liquid water expressed by the relative saturation RSS (–) according to Eqn. 4.36 (see Illangasekare et al., 1990).

$$M_{flow} = k_{sat,snow} \cdot RSS^3 \qquad (4.36)$$

The dimensionless relative saturation RSS is defined as the relative saturation in excess of water retained

by capillary forces (Illangasekare et al., 1990; Tarboton and Luce, 1996) and can be computed as:

$$RSS = \frac{\text{liquid vol.} - \text{capillary retention vol.}}{\text{pore vol.} - \text{capillary retention vol.}} \quad (4.37)$$

Tarboton and Luce (1996) relate the capillary retention volume to the water equivalent of the solid matrix given by $SWE \cdot (1 - SLF)$. Thus, the whole Eqn. 4.37 needs to be divided by this expression. For the single terms we obtain:

Capillary retention volume

$$= \frac{\text{capillary retention volume}}{SWE \cdot (1 - SLF)}$$

$$= SCR = \text{const.}$$

Tarboton and Luce (1996) suggest a value of 0.05 for the newly introduced constant SCR.

Liquid volume

$$= \frac{\text{liquid water volume}}{SWE \cdot (1 - SLF)}$$

$$= \frac{SWE \cdot SLF}{SWE \cdot (1 - SLF)}$$

$$= \frac{SLF}{1 - SLF}$$

Pore volume

$$= \frac{\text{pore volume}}{SWE \cdot (1 - SLF)}$$

$$= \frac{\text{snow volume} - \text{solid water volume}}{SEC \cdot (1 - SLF)}$$

$$= \frac{\left(\dfrac{\text{mass of snow}}{\rho_{snow}}\right) - \left(\dfrac{\text{mass of ice}}{\rho_i}\right)}{SEC \cdot (1 - SLF)}$$

$$= \frac{\left(\dfrac{SWE \cdot \rho_w}{\rho_{snow}}\right) - \left(\dfrac{SEC \cdot (1 - SLF) \cdot \rho_w}{\rho_i}\right)}{SEC \cdot (1 - SLF)}$$

$$= \frac{1}{1 - SLF} \cdot \frac{\rho_w}{\rho_{snow}} - \frac{\rho_w}{\rho_i}$$

Collecting together all terms, Eqn. 4.37 becomes Eqn. 4.38.

$$RSS = \frac{\left(\dfrac{SLF}{1 - SLF}\right) - SCR}{\left(\dfrac{1}{1 - SLF} \cdot \dfrac{\rho_w}{\rho_{snow}}\right) - \left(\dfrac{\rho_w}{\rho_i}\right) - SCR}$$

$$(4.38)$$

Eqn. 4.38 is identical to Equation 48 in Tarboton and Luce (1996) except for the term $1/(1 - SLF)$ in the denominator. The reason is that, although not explicitly stated, Tarboton and Luce (1996) define ρ_{snow} in their equation 48 to be the *dry snow density*, $\rho_{snow,dry}$, which, as opposed to the common snow density ρ_{snow}, relates only for the mass of solid water to the snow volume and thus neglects the mass of liquid water (see Equation 7 in Morris and Kelly, 1990).

Recalling Eqn. 4.11 from Sec. 4.1.2.5, the equality between $(1 - SLF) \cdot \rho_{snow}$ and $\rho_{snow,dry}$ can be demonstrated

$$\rho_{snow,dry} = \frac{m_i}{v_s}$$

$$= \frac{m_i \cdot m_s}{v_s \cdot m_s}$$

$$= \rho_{snow} \cdot \frac{m_i}{m_s}$$

$$= \rho_{snow} \cdot \frac{m_s - m_w}{m_s}$$

$$= \rho_{snow} \cdot \left(1 - \frac{m_w}{m_s}\right)$$

$$= \rho_{snow} \cdot (1 - SLF)$$

where m_i, m_w, and m_s (kg) represent masses of ice (solid), water (liquid), and snow (mixture of solid and liquid), respectively, and v_s (m^3) is the corresponding snow volume. Using $\rho_{snow,dry}$, Eqn. 4.38 may be rewritten as Eqn. 4.39 which is identical to Equa-

tion 48 in Tarboton and Luce (1996). They suggest for $\rho_{snow,dry}$ a value of 450 kg/m^3.

$$RSS = \frac{\left(\dfrac{SLF}{1 - SLF}\right) - SCR}{\left(\dfrac{\rho_w}{\rho_{snow,dry}}\right) - \left(\dfrac{\rho_w}{\rho_i}\right) - SCR} \quad (4.39)$$

All in all, the rate of melt water outflow M_{flow} is controlled by the three free parameters listed in Table 4.4.

Table 4.4: *Parameters controlling the rate of meltwater outflow. Approximate values in brackets after* Tarboton and Luce (1996)*.*

Symbol	Units	Description
$k_{sat,snow}$	m/s	Saturated hydraulic conductivity. To be calibrated.
SCR	–	Capillary retention volume as a fraction of the solid water equivalent. [≈ 0.05].
$\rho_{snow,dry}$	kg/m^3	Snow dry density [≈ 450].

4.1.6   Test application

The energy balance model has been tested on daily data from two mountains in Germany. The two sites are 'Kahler Asten' (Lat: 51.1814, Lon: 8.4897, Elevation: 839 m) and 'Fichtelberg' (Lat: 50.4294, Lon: 12.9553, Elevation: 1213 m). Note that coordinates are in decimal degrees.

The required meteorological data were supplied by the German Weather Service (DWD) free of charge via the 'WEBVERDIS' interface. The data are in daily resolution and some post-processing was necessary to identify gaps and to remove duplicate records. Based on the data from the two mentioned sites, a common parameter set has been identified (Table 4.5) by carrying out a sequence of Monte-Carlo simulations with successive narrowing of the sampling ranges.

A comparison of the observed and simulated snow water equivalent for the two test sites is provided in Figs. 4.7 & Fig. 4.8. Note that only a selection of the data was used for model calibration. In particular, the focus was put on the melting phase since this is of special interest for flood forecasting.

Table 4.5: *Calibrated parameters of the energy balance snow model based on daily data from two sites in Germany (Fichtelberg and Kahler Asten).*

Parameter	Value	Corresp. eqn.(s)
T_{crit}	0.2	Eqn. 4.12
μ	0.35	Eqn. 4.9
$a0$	0.002	Eqn. 4.30
$a1$	0.0008	Eqn. 4.30
ε_{min}	0.84	Eqn. 4.24
ε_{max}	0.99	Eqn. 4.24
$\rho_{snow,dry}$	450	Eqn. 4.39
$k_{sat,snow}$	4.0e-05	Eqn. 4.36
SCR	0.05	Eqn. 4.39
AS_{min}	0.55	Eqn. 4.17
AS_{max}	0.88	Eqn. 4.17
$k_{AS}(TA \geq 0)$	1.11e-06	Eqn. 4.17
$k_{AS}(TA < 0)$	4.62e-07	Eqn. 4.17
D_s	0.1	Eqn. 4.3
ρ_s	1300	Eqn. 4.3
C_s	2.18	Eqn. 4.3

4.2   Degree-day method

This method is currently *not* implemented in an any `echse`-based hydrological models.
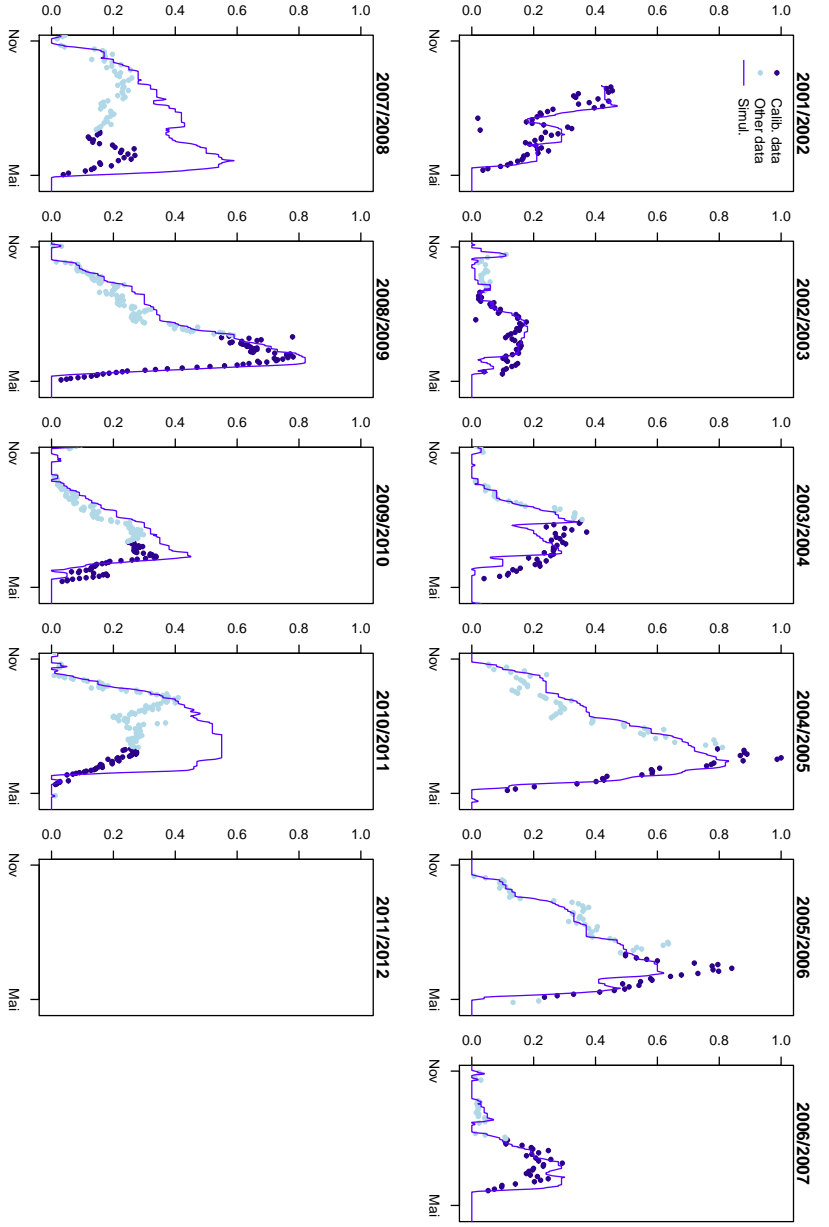
Figure 4.7: *Observed and simulated snow water equivalent at DWD station 'Fichtelberg'.*
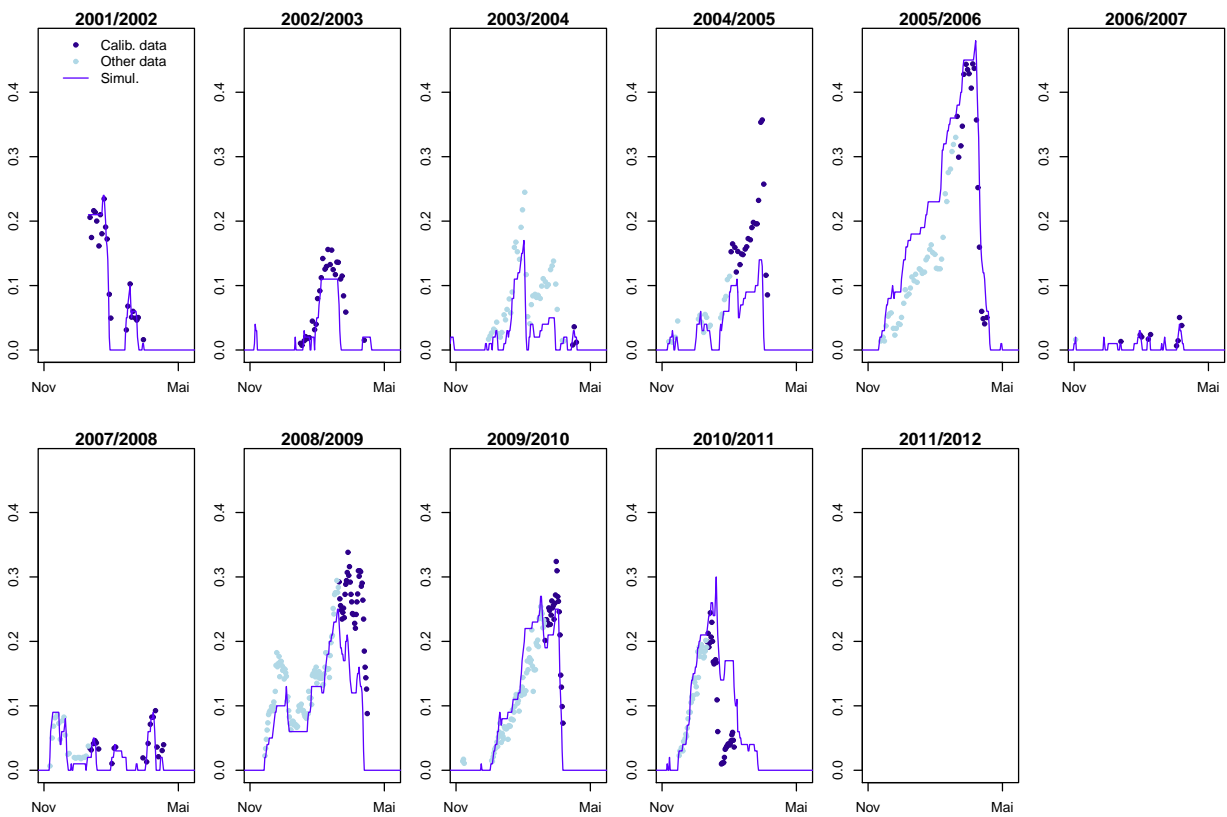
Figure 4.8: *Observed and simulated snow water equivalent at DWD station 'Kahler Asten'.*

Chapter 5

Runoff generation

5.1 Introduction

To avoid confusion, it is important to distinguish between the terms *runoff generation* and *runoff concentration*. As *runoff generation*, we understand the transformation of water input (rain, snow melt) into runoff *at the local scale*, i. e. at every single point of a catchment. In contrast to that, the term *runoff concentration* describes the transport of the locally generated runoff to the catchment's outlet (or the nearest river).

In some cases, the strict separation of the two terms is really pragmatic. However, it provides a clear and quite useful concept for hydrological catchment modeling.

5.2 Simple four components model

5.2.1 Processes and equations

The four components runoff generation model described here is based on the concepts used in the LARSIM[1] model Ludwig and Bremicker (2006). Originally, most equations were first presented by Todini (1996).

The runoff generation model is built upon the water balance of a soil column (Fig. 5.1) which can be expressed by Eqn. 5.1

$$\frac{d\theta}{dt} = \frac{WS - r_{surf} - r_{pref} - r_{int} - r_{base} - r_{evap}}{D}$$

$$(5.1)$$

with

---

[1] Model variant '4Q-KOMP mit A2'

θ	(–)	Soil water content as m^3/m^3
WS	(m/s)	Rate of water supply (see Eqn. 5.2)
r_{surf}	(m/s)	Rate of surface runoff
r_{pref}	(m/s)	Rate of quick sub-surface runoff (preferential flow)
r_{int}	(m/s)	Rate of slow sub-surface runoff (interflow)
r_{base}	(m/s)	Rate of deep percolation (rate of ground water recharge)
r_{evap}	(m/s)	Rate of evapo(transpi)ration
D	(m)	Depth (thickness) of soil column.

The relevant thickness of the soil column D is equivalent to the rooted depth. Soil water at greater depths is assumed (1) to be unavailable for evapotranspiration and (2) not to contribute to lateral runoff processes.

Snow coverage of the soil column is assumed to be either 0 or 100%, i. e. partial covering is *not* simulated. As long as no snow is present, the rate of water supply to the soil column is the same as the intensity of precipitation, PI. Once a snow cover exists, all precipitation is trapped in the snow and the rate of water supply is controlled by the melt rate, r_{melt} (Eqn. 5.2). Both PI and r_{melt} are in units of m/s.

$$WS = \begin{cases} r_{melt} & \text{if snow cover is present} \\ PI & \text{else} \end{cases} \quad (5.2)$$

In the presented four components model, the generation of direct runoff[2] is bound to the existence of (local) soil saturation. Thus, the model accounts for surface runoff due to infiltration excess but *not* for Hortonian surface runoff.

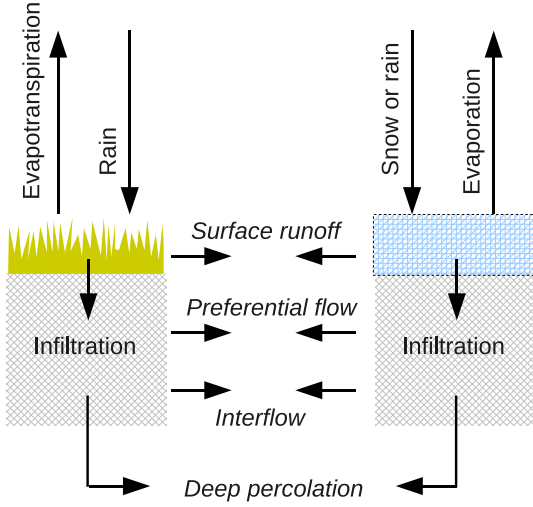[2] Runoff being quickly generated in response to water input.

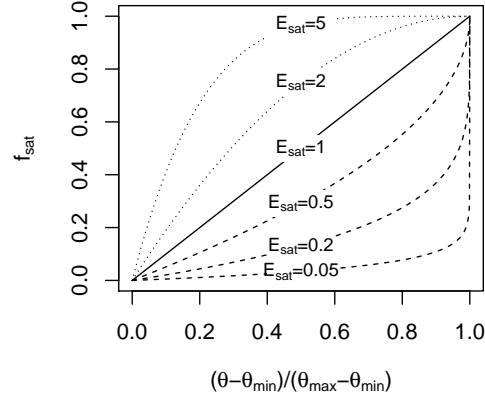**Figure 5.1:** *Water fluxes with respect to a soil column with (right) and without snow cover (left).*

Figure 5.2: *Influence of the empirical parameter β on the relation between the catchment-integrated relative filling of the soil reservoir (x-axis) and the fraction of saturated areas f_{sat} (y-axis). Only values of $\beta \leq 1$ are physically reasonable.*

Following to the Xinanjiang approach (Zhao et al., 1980), the fraction of saturated areas f_{sat} in a catchment can be estimated from the area-integrated relative saturation of the soil S which is the ratio of the current and maximum soil water content θ and θ_{max}, respectively (Eqns. 5.3 and 5.4). The rationale of the Xinanjiang model is a positive correlation between the catchment's average wetness, represented by the relative filling of the soil reservoir and the proportion of saturated areas. In other words, the occurrence of local saturation is assumed to increases as the catchment's average wetness becomes higher.

$$S = \frac{\theta}{\theta_{max}} \tag{5.3}$$

$$f_{sat} = 1 - (1 - S)^{\beta} \tag{5.4}$$

The shape of the relation between S and f_{sat} is controlled by a dimensionless empirical parameter β. The effect of different values of β is illustrated in Fig. 5.2. A linear relation is assumed in the case $\beta = 1$. Note that only values of $\beta \leq 1$ are physically reasonable. Max

The amount of direct runoff h_d (in meters) is computed as a function of the fraction of saturated areas f_{sat} according to Eqn. 5.5

$$h_d = \begin{cases} I - (W_m - W) + W_m \cdot x^{\beta+1} & if(x > 0) \\ I - (W_m - W)) & if(x \leq 0) \end{cases}$$

with

$$x = \left(1 - \frac{W}{W_m}\right)^{\left(\frac{1}{\beta+1}\right)} - \frac{I}{(1+\beta) \cdot W_m} \tag{5.5}$$

and I being the total water input in a time step ($I = WS \cdot \Delta t$), W being the amount of water in the modeled soil column ($W = \theta \cdot D$) and W_m being the maximum capacity of the soil column ($W_m = \theta_{max} \cdot D$), all in units of meters. The derivation of this expression can be found in Todini (1996) but is has to be noted that in this publication some signs are incorrect. The corrected version is presented in Bremicker et al. (2006), for example. The relation between h_d and I according to Eqn. 5.5 is illustrated in Fig. 5.3 for fix values of W and W_m. A retention effect is visible for small to moderate water inputs. For water inputs considerably higher than the initial storage capacity of the soil, the relation between h_d and I becomes linear.

The model described here distinguished two components of direct runoff which differ with respect to retention characteristics. They may be considered as surface runoff and quick subsurface runoff through preferential flow paths. The proportion of the two components is controlled by a threshold value thr_{surf} in units of m/s.
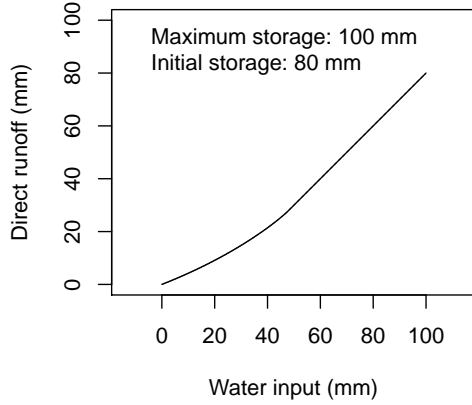
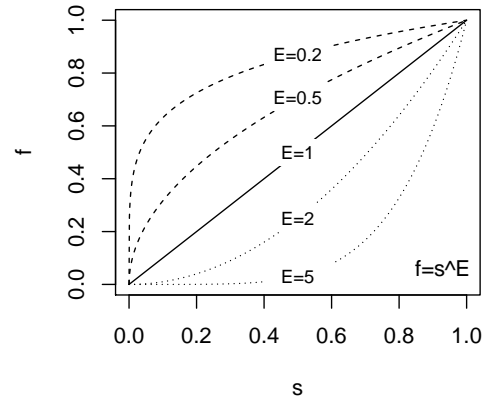**Figure 5.3:** *Direct runoff computed with Eqn. 5.5 for example values of soil storage and water input.*

Figure 5.4: *Effect of the exponent E in a formula $f = s^E$ for s in range [0,1].*

The rates of surface runoff and quick subsurface runoff are computed according to Eqn. 5.6 and Eqn. 5.7

$$r_{surf} = max\left(0, \frac{h_d}{\Delta t} - thr_{surf}\right) \qquad (5.6)$$

$$r_{pref} = \frac{h_d}{\Delta t} - r_{surf} \qquad (5.7)$$

Thus, if the rate of direct runoff production $h_d/\Delta t$ is below the threshold thr_{surf}, only subsurface runoff is generated. Otherwise, surface runoff is generated from the excessive water. Note that the settings $thr_{surf} = 0$ or $thr_{surf} \to \infty$ effectively result in a model with only 3 runoff components.

The generation of the slow runoff components is closely linked to the relative saturation of the soil S (Eqn. 5.3). The rate of interflow runoff is computed by Eqn. 5.8 using three empirical parameters. Here, b_{int} represents a maximum rate of interflow runoff generation corresponding to total saturation of the soil. The actual rate, r_{int}, decreases at lower values of the soil saturation. If the saturation falls below a threshold level S_{int}, no interflow runoff is generated at all. The shape of the soil moisture dependence is controlled by the empirical exponent E_{int} whose effect is illustrated in Fig. 5.4 (argument s represents the fractional expression of Eqn. 5.8). The higher the value of the empirical exponent, the wetter the soil needs to be for interflow

runoff becoming an important component. At very low values of E_{int}, interflow runoff is produced almost at the maximum rate b_{int}, as soon as the soil saturation exceeds the threshold S_{int}. As in LARSIM, the parameter E_{int} is treated as a constants with a value of 1.5 (Bremicker et al., 2006).

$$r_{int} = \begin{cases} b_{int} \cdot \left(\frac{S - S_{int}}{1 - S_{int}}\right)^{E_{int}} & \text{if } S > S_{int} \\ 0 & \text{if } S \leq S_{int} \end{cases} \qquad (5.8)$$

The rate of groundwater recharge (or base flow runoff), r_{base}, is computed by Eqn. 5.9 which is conceptually identical to Eqn. 5.8. Here, b_{base} is the maximum rate of groundwater recharge which corresponds to a saturated soil. If the relative saturation of the soil falls below S_{base}, the rate of groundwater recharge becomes zero. The shape of the dependence between r_{base} and S is controlled by the empirical exponent E_{base}. Again, the effect of this exponent can be seen from Fig. 5.4 (argument s represents the fractional expression of Eqn. 5.9). As in LARSIM, the parameters S_{base} and E_{base} are treated as a constants with values of 0.05 and 1, respectively (Bremicker et al., 2006). Thus, only b_{base} remains as a calibration parameter.

$$r_{base} = \begin{cases} b_{base} \cdot \left(\frac{S - S_{base}}{1 - S_{base}} \right)^{E_{base}} & \text{if } S > S_{base} \\ 0 & \text{if } S \leq S_{base} \end{cases}$$
$$(5.9)$$

Of course, the theory described so far is only applicable to areas where soil water storage occurs. For areas covered by water or impervious surfaces, the rate of surface runoff r_{surf} equals the rate of rainfall or snow melt, respectively.

5.2.2   Combination with other models

Depending on the model's purpose and local conditions, the described runoff generation model has to be augmented with

- a model to compute snow storage and melt,

- a model to estimate evapotranspiration,

- an approach for precipitation correction (if not done externally).

5.2.3   Mathematical solution

Eqn. 5.1 is an ordinary differential equation. Depending on the use of the model, a more of less sophisticated numerical solution has to be adopted. If computation times are critical (e. g. in operational models), a simple 1st order numerical solution may be preferable. Then, however, it needs special efforts to prevent unstable or unphysical solutions. In particular, in the absence of appropriate correction terms, a 1st oder solution of Eqn. 5.1 may yield a computed soil moisture θ which is negative.

5.2.4   Implementation

Table 5.1 relates the identifier names used in the model implementation (names of state variables and parameters) to the symbols used in the process equations (Sec. 5.2.1). Additional information that may be helpful when calibrating a model without any prior knowledge of parameter values is given in Sec. 5.2.5.

5.2.5   Hints for application

The parameter b_{base} specifies the rate of deep percolation under the conditions of a fully saturated soil
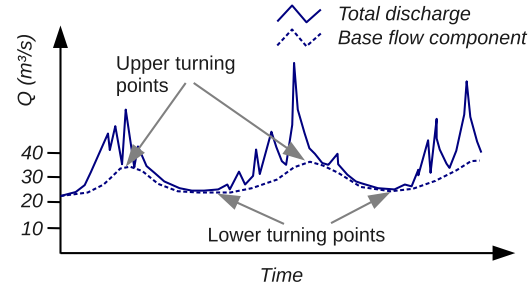

Figure 5.5: *Discharge hydrograph with manually separated base flow component.*

(Eqn. 5.9). At a first glance, it seems as if b_{base} could be estimated from the soil's saturated hydraulic conductivity k_f. However, at high values of the soil moisture, the other runoff components are also active and, typically, these other components are much more effective in draining the soil. Consequenty, we can expect $b_{base} \ll k_f$.

A more promising approach to estimate b_{base} relies on the analysis of a discharge hydrograph (Fig. 5.5). In this figure, an approxiate hydrograph of the base flow component was added. It can be drawn by hand as a smooth line connecting the annual minimum values (low flows) also touching the minima during the rainy season. Obviously, the hydrograph of the base flow component has, like any periodic function, two types of turning points. For convenience, we focus on the lower turning points here. They are easier to identify from the data without the need for any drawing, actually.

In the following we assume that the base flow component is equivalent to the outflow from a conceptual ground water reservoir. For simplicity, we may consider a linear reservoir described by Eqns. 6.1 & 6.2 (see page 47). From the differential equation, we find that, at the mentioned turning points, the derivative of the storage volume with respect to time becomes zero, hence the rates of inflow and outflow are equal. Consequently, the *base flow rate* at the turning points in a plot like Fig. 5.5 directly yields an estimate of the *rate of ground water recharge*, r_{base}, at the respective point in time.

The relation between the actual rate of ground water reacharge r_{base} and the model parameter b_{base} is given by Eqn. 5.9. This can be rearranged and r_{base} can be substituted by $A \cdot Q_{base}$ where A is the size of the catchment in units of m^2 and Q_{base} is the base flow component in m^3 s^{-1} (Eqn. 5.10). Using the fixed val-

Table 5.1: *Symbols used in the process equations (Sec. 5.2.1), corresponding identifiers, and hints for calibration.*

Symbol	Identifier	Units	Typical values	Details
θ	wc	–	–	Computed state variable
D	soildepth	m	Rooted depth	–
θ_{max}	wc_max	–	0.4–0.5	Table 9.1 on page 59
β	exp_satfrac	–	0.01–1	See Fig. 5.2
thr_{surf}	thr_surf	m/s	–	Values of 0 or near ∞ result in a 3 components model (see Eqns. 5.6 & 5.7).
S_{int}	relsat_inter	–	0.5 – 0.8	Number between 0 and 1.
r_{int}	rate_inter	m/s	example: 1.e-07	Depends on hydraulic conductivity
r_{base}	rate_base	m/s	example: 1.e-08	Depends on hydraulic conductivity

ues of S_{base} and E_{base} mentioned in Sec. 5.2.1, we end
up with Eqn. 5.11.

$$b_{base} = \frac{Q_{base}}{A} \cdot \left(\frac{S - S_{base}}{1 - S_{base}} \right)^{-E_{base}} \qquad (5.10)$$

$$= \frac{Q_{base}}{A} \cdot \left(\frac{0.95}{S - 0.05} \right) \qquad (5.11)$$

In order to calculate b_{base} from Eqn. 5.11 we have to
supply an estimate of the soil saturation S at the respec-
tive point in time (i. e. the analyzed turning point). For
the lower turning points, a reasonable guess can be ob-
tained from the soil water content at the wilting point.
For a silty soil, for example, the saturation S would
be ≈ 0.2 for a soil moisture at the wilting point of 0.1
and a maximum water content of 0.48 (see Table 9.1 on
page 59).

The value of b_{base} obtained from the hydrograph
analysis is a crude estimate. However, it might help in
the definition of a proper search range for b_{base} in the
context of automatic model calibration.
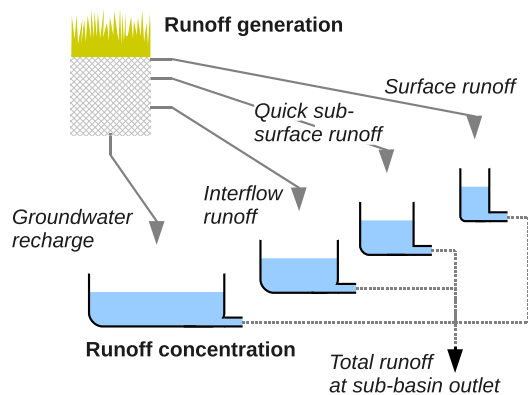
Chapter 6

Runoff concentration

Figure 6.1: *Parallel storage model for the case of four runoff components.*

6.1 Introduction

The term *runoff concentration* describes the transport of the locally generated runoff (see Chap. 5) to the catchment's outlet or the nearest river. In general, the description of water transport covers the phenomena of translation and retention.

6.2 Parallel storage model

6.2.1 Processes and equations

In the parallel storage model, it is assumed that runoff concentration can be computed separately for the individual runoff components. For each component, translation and retention is simulated by means of a simple reservoir model. The cumulated runoff from the parallel reservoirs finally represents the sub-basins total runoff (Fig. 6.1).

Following the approach used in LARSIM (Ludwig and Bremicker, 2006), all reservoirs depicted in Fig. 6.1 are of the linear type. Thus, in addition to the mass balance (Eqn. 6.1), the linear relation of Eqn. 6.2 applies to each reservoir.

$$\frac{dv}{dt} = q_{in} - q_{out} \qquad (6.1)$$

v	Storage volume	L^3
q_{in}	Inflow rate	L^3/T
q_{out}	Outflow rate	L^3/T

$$q_{out} = \frac{1}{k} \cdot v \qquad (6.2)$$

k Retention constant T

Eqns. 6.1 and 6.2 can be combined and integrated over time using the substitution method. Assuming that the inflow rate q_{in} is constant over a discrete time step, the integration yields Eqn. 6.3 as the solution for the storage volume.

$$v(t_0 + \Delta t) = (v(t_0) - q_{in} \cdot k) \cdot e^{(-\Delta t/k)} + q_{in} \cdot k \quad (6.3)$$

$v(t_0)$	Initial storage at	L^3
Δt	Length of time step	T

The only parameters in this runoff concentration model are the values of the retention constants k (one for each reservoir shown in Fig. 6.1. Regarding these constants, we can formulate two expectations:

1. Larger values of k result in a higher retention effect and thus in a more delayed input-output reaction (Fig. 6.2). Consequently, we expect the highest k value for the groundwater reservoir while the smallest k value corresponds to the reservoir describing the concentration of surface runoff.
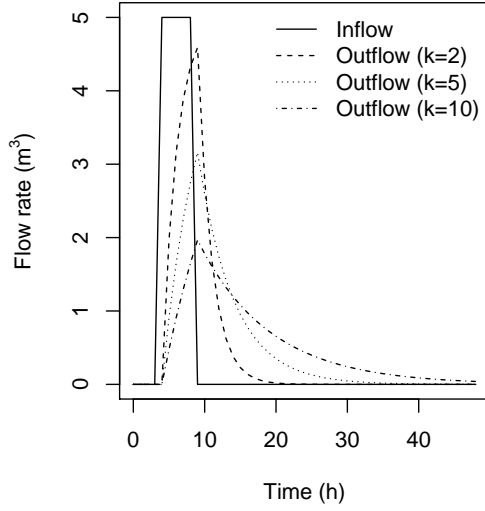
Figure 6.2: Outflow hydrographs from a single linear reservoir for an identical input signal but different storage constants k (hours).

2. Furthermore, it seems legitimate to assume a relation between the k values and the characteristics of a sub-basin. In particular, we expect smaller retention constants in regions with steep hill slopes, dense drainage networks, and for sub-basin of compact shape.

To take these two aspect into account, it is convenient to define the retention constants as in Eqns. 6.4 to 6.7.

$$\text{Surface runoff:} \qquad k = S_{surf} \cdot CTI \qquad (6.4)$$

$$\text{Preferential flow:} \qquad k = S_{pref} \cdot CTI \qquad (6.5)$$

$$\text{Interflow:} \qquad k = S_{inter} \cdot CTI \qquad (6.6)$$

$$\text{Base flow:} \qquad k = S_{base} \cdot CTI \qquad (6.7)$$

Here, S_{surf}, S_{pref}, S_{inter}, and S_{base} are dimensionless calibration parameters, fulfilling $S_{surf} < S_{pref} < S_{inter} < S_{base}$ (recall 1st point of above enumeration). Furthermore, CTI is an indicator of the sub-basin's runoff concentration characteristics having the dimension of a time (2nd point of above enumeration). For estimating the CTI different approaches do exist. In LARSIM (Ludwig and Bremicker, 2006), for example, an empirical formula derived by Kirpich (1940) is used. This one computes the CTI from the average length

and slope of the major reach(es) in a sub-basin. Alternatively, a CTI can be derived by analysis of a digital elevation model. This approach is described in the documentation of the **topocatch** preprocessor (see Kneis, 2012a).

See Sec. 6.2.4 for the relation between the k values and the half-life time τ.

The inflow rate q_{in} (m³/s) appearing in Eqns. 6.1 to 6.3 is generally obtained by multiplying the runoff rate (m/s) by the contributing area (m²). For the reservoir describing the concentration of surface runoff, q_{in} is usually composed of the runoff generated on saturated soils, water surfaces, and also impervious surfaces.

6.2.2   Mathematical solution

In each time step, the storage of the four reservoirs is updated based on Eqn. 6.3 using the individual inflow rates and retention constants (Eqns. 6.4 to 6.7). The total outflow from a sub-basin is then obtained as the sum of the outflow rates from the four linear reservoirs.

Note that, if Eqn. 6.2 is applied to the already updated storage volumes, the computed outflow rates are *instantaneous values* which correspond to the *end* of a time step. To ensure conservation of mass, these rates should not be directly used as inputs for a downstream model (usually a flow routing model). Instead, *time-step averaged* outflow rates must be passed to the downstream model. For each reservoir, the time-step averaged outflow rates are obtained from the discrete version of the mass balance equation (recall Eqn. 6.1) as shown in Eqn. 6.8.

$$\overline{q_{out}} = q_{in} - \frac{v(t_0 + \Delta t) - v(t_0)}{\Delta t} \qquad (6.8)$$

$\overline{q_{out}}$	Time-step averaged outflow rate	L³/T
q_{in}	Inflow rate (constant over Δt)	L³/T
$v(t_0)$	Initial storage volume	L³
$v(t_0 + \Delta t)$	Storage at end of time step	L³

6.2.3   Implementation

Table 6.1 relates the identifier names used in the model implementation (names of state variables and parameters) to the symbols used in the process equations (Sec. 6.2.1).

Table 6.1: *Symbols used in the process equations (Sec. 6.2.1) and corresponding identifiers.*

Symbol	Identifier	Units	Details
v (surface runoff)	`vol_surf`	m^3	Storage volume of surface runoff reservoir
v (preferential flow)	`vol_pref`	m^3	Storage volume of preferential flow reservoir
v (interflow)	`vol_inter`	m^3	Storage volume of interflow reservoir
v (baseflow)	`vol_base`	m^3	Storage volume of baseflow reservoir
S_{surf}	`str_surf`	sec	Retention constant of surface runoff reservoir
S_{pref}	`str_pref`	sec	Retention constant of preferential flow reservoir
S_{inter}	`str_inter`	sec	Retention constant of interflow reservoir
S_{base}	`str_base`	sec	Retention constant of baseflow reservoir

6.2.4   Hints for application

As with all state variables, initial values must be assigned to the storage volumes listed in Table 6.1. These values are generally unknown and cannot be derived from observation data. Therefore, a widely used approach is to simply guess the initial values and to allow for a rather long 'warm-up' period of the model (several years). If boundary condition data are available for a limited period of time only, one should run a sequence of warm-up simulations. Guessed initial values are used only in the first run. In all later runs, the model is initialized with the final state of the previous run. The success of the latter strategy can be checked, for example, by plotting some simulated hydrographs. If the differences between the hydrographs of consecutive runs becomes negligible, the desired equilibrium of the storage volumes has been reached. However, even then, the initial part of a simulated time series should not be compared to observations because the initial state is still a (refined) guess.

The retention constants listed in Table 6.1 need to be identified by calibration. The values depend on the characteristics of the modeled basin, the model's resolution, as well as on the definition of the used concentraction time index, CTI (see Eqns. 6.4 to 6.7). When calibrating the retention constants, one should keep in mind that a particular parameter set is reasonable only if $S_{surf} < S_{pref} < S_{inter} < S_{base}$ (see Sec. 6.2.1 for details).

The time for model calibration can be reduced (and the overall chance of success can be increased), if prior knowledge on the magnitude of the retention constants is available. If a calibrated model for another nearby basin is available, one could try to adopt the values used in this model as initial guesses. However, this will only work if the basins' characteristics in terms of climate, geomorphology, and land-use are really comparable. Furthermore, the two models must also be comparable with respect to the spatial and temporal discretization.

If another model for a nearby basin is not available or the mentioned conditions are not met, one can try to infer estimates of the retention constants from observed discharge hydrographs. For that purpose, one has to analyze the shape of stream flow recessions using the theory of the single linear reservoir.

Substituting the volume v in Eqn. 6.3 using Eqn. 6.2 yields an equation to predict the future outflow of a linear reservoir using a known initial outflow rate (Eqn. 6.9).

$$q_{out}(t_0 + \Delta t) = (q_{out}(t_0) - q_{in}) \cdot e^{(-\Delta t/k)} + q_{in} \quad (6.9)$$

During recession some time after a flow peak, we can assume that the outflow from the reservoir is much higher than the inflow. Assuming zero inflow, Eqn. 6.9 simplifies to Eqn. 6.10

$$q_{out}(t_0 + \Delta t) = q_{out}(t_0) \cdot e^{(-\Delta t/k)} \quad (6.10)$$

which can then be solved for the storage constant k (Eqn. 6.11). Note that all values appearing at the right hand side of this equation are easily obtained from a hydrograph plot (Fig. 6.3).

$$k = \frac{\Delta t}{ln(q_{out}(t_0)/q_{out}(t_0 + \Delta t))} \quad (6.11)$$

When using Eqn. 6.11 to estimate the model parameters S_{surf}, S_{pref}, S_{inter}, and S_{base}, one must to take Eqn. 6.4–6.7 into account. Thus, the values of k computed from Eqn. 6.11 have to be divided by the concentration time index CTI in order to obtain the desired values of S_{surf}, S_{pref}, S_{inter}, and S_{base}.
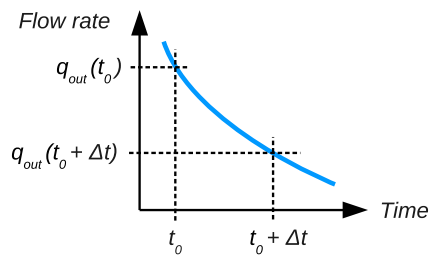
Figure 6.3: *Analysis of the recession following a flow peak.*

In practice, the estimation of the storage constants is complicated by the fact that multiple runoff components contribute to stream flow at the same time. Thus, to estimate the value of a particular constant, one has to consider a recession which is likely to be *dominated* by the corresponding process. For example, S_{pref} and possibly S_{surf} (and possibly S_{inter}) are likely to control the steep part of the recession after major events. To identify S_{base}, however, one needs analyze long-lasting recessions, preferably at the end of a rainy season.

In general, the obtained values for S_{surf}, S_{pref}, S_{inter}, and S_{base} should be considered as rough estimates only. It is recommended to refine the estimates during calibration.

Chapter 7

Channel flow

7.1 Introduction

This chapter desribes approaches to the simulation of open channel flow. In a dynamic model, we generally deal with unsteady flow conditions. One can distinguish between two basic concepts:

Hydrodynamic approach Such models are based on a solution of the St. Venant equations, expressing the conservation of momentum and mass. The solution of these (possibly simplified) partial differential equations requires rather expensive numerical methods.

Hydrological approaches Such models still consider the principle of mass conservation (continuity equation). However, in contrast to hydrodynamic models, they do not account for the conservation of momentum or energy but rely on empirical relations between channel storage and flow.

In hydrological catchment models, hydrological approaches are widely because they are easier to implement and allow for fast computations based on anaytical solutions. Prominent examples include:

- the single reservoir approach,
- the Muskingum method,
- the method of Kalinin-Miljukov (Nash's cascade).

The approach(es) described below apply to a single reach. Here, a reach is defined as a river section of a constant geometry (i. e. cross-section and slope). In hydrological catchment modeling for larger areas, cross-section and slope data are usually scarce and a constant geometry is therefore assumed between the neighbored junctions along a river. Then, a reach is practically identical to the river section between two junctions.
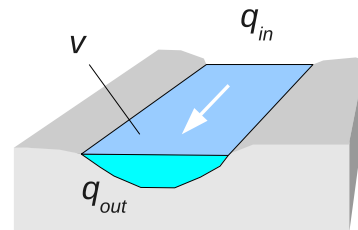
Figure 7.1: *Sketch of a reach with storage volume v, and the rates of in- and outflow (q_{in}, q_{out}).*

7.2 Single reservoir approach

7.2.1 Processes and equations

In this approach, a reach (Fig. 7.1) is treated as a single reservoir. Considering the principle of mass conservation, the storage volume v (m^3) is related to the rates of inflow q_{in} and outflow q_{out} (both in m^3/s) by the continuity equation Eqn. 7.1.

$$\frac{dv}{dt} = q_{in} - q_{out} \qquad (7.1)$$

To simulated the dynamics of v for a given inflow rate, the continuity equation must be complemented by a second equation relating q_{out} to v. In the case of a linear reservoir, for example, this missing relation is given by Eqn. 7.2 where k is a retention constant with the dimension of a time. The advantage of this linear relation is that it allows for an analytical solution of Eqn. 7.1.

$$q_{out} = \frac{1}{k} \cdot v \qquad (7.2)$$

Assuming that the inflow rate q_{in} is constant over a discrete time step of length Δt, combining Eqn. 7.1

51

and 7.2 and subsequent integration using the substitution method yields Eqn. 7.3.

$$v(t_0 + \Delta t) = (v(t_0) - q_{in} \cdot k) \cdot e^{(-\Delta t/k)} + q_{in} \cdot k \quad (7.3)$$

$v(t_0)$	Initial storage at	L^3
Δt	Length of time step	T

A slightly advanced version of the linear reservoir model is obtained if the inflow rate q_{in} is allowed to vary linearly with time. Then, the modified continuity equation is given by Eqn. 7.4

$$\frac{dv}{dt} = q_{in,0} + (q_{in,1} - q_{in,0}) \cdot t - q_{out} \quad (7.4)$$

where $q_{in,0}$ and $q_{in,1}$ represent an initial and final inflow rate, respectively. After combining Eqn. 7.4 with Eqn. 7.2, the integration yields Eqn. 7.5

$$v(t_0 + \Delta t) = v(t_0) \cdot x + \frac{a \cdot (x-1)}{b^2} \quad (7.5)$$

$$+ \frac{q_{in,0} \cdot (x-1) - a \cdot \Delta t}{b}$$

with the abbreviations

$$a = (q_{in,1} - q_{in,0})/\Delta t$$

$$b = -1/k$$

$$x = e^{(-\Delta t/k)}$$

and

$$q_{in,0} = q_{in}(t_0)$$

$$q_{in,1} = q_{in}(t_0 + \Delta t)$$

This equation is also used in the LARSIM model (same as Equation 3.54 in Ludwig and Bremicker, 2006).

Unfortunately, for natural channels, the relation between q_{out} and v is typically non-linear and Eqn. 7.2 is therefor not applicable. However, the analytical solution of the linear reservoir equation (Eqns. 7.3 or 7.5) is very attractive to use because of its low computational cost. A common solution to this problem is the idea of
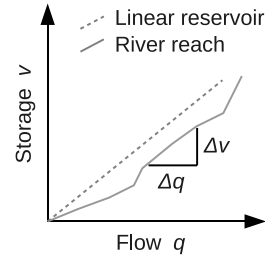
Figure 7.2: *Relation between storage volume v and outflow rate q_{out} for a linear reservoir and a river reach.*

a locally-linear reservoir. In this concept, the analytical solution of the linear reservoir equation is still used but the retention constant k is allowed to depend on the storage volume v (or the outflow rate q_{out}).

According to Eqn. 7.2, the retention constant of a linear reservoir is given by Eqn. 7.6

$$k = \frac{v}{q_{out}} \quad (7.6)$$

.

Similarly, for the locally-linear reservoir, the retention constant is given by Eqn. 7.7

$$k = \frac{\Delta v}{\Delta q_{out}} \quad (7.7)$$

.

Thus, the retention constant k still equals the slope of the relation between v and q_{out} (Fig. 7.2).

For channels of known geometry, the relation between q_{out} to v (Fig. 7.2) can be derived from a rating curve, i. e. corresponding observations of flow rates and water levels (the latter being convertable to storage volumes). Since the vast majority of simulated reaches in a hydrological model is ungaged, rating curves are not practically available and need to be estimated. This is usually done by applying Manning's equation (Eqn. 7.8).

$$q(h) = \frac{1}{n} \cdot \sqrt{S_f} \cdot R(h)^{2/3} \cdot A(h) \quad (7.8)$$

q	Flow rate	m^3/s
S_f	Slope of the energy grade line	–
R	Hydraulic radius	m
A	Wet cross-section area	m^2
h	Water level	m
n	Manning's n (parameter)	Non-physical

Considering that the storage volume v in a uniform reach equals $A \cdot L$ (L: length of the channel), Eqn. 7.8 can be used to tabulate corresponding pairs of v and q_{out} and thus also $k(q_{out})$ or $k(v)$, respectively (recall Eqn. 7.7). The required information are:

- The functions $A(h)$ and $R(h)$. They can easily be computed from the x-section's geometry (table of offsets and corresponding elevations).

- The roughness parameter n. Tables and empirical formulas exist to estimate this value from channel properties. It can also be fitted by steady flow modeling.

- The slope of the energy grade line S_f. In practice, only the slope of the channel bottom S_0 is constant and known. It can be measured in the field or has to be gathered from a digital elevation model (with subsequent quality checks).

7.2.2   Mathematical solution

Governing equation

In each time step, the storage v is updated using Eqn. 7.5. The applied retention constant is an average value ($\overline{k}$) taking into account the initial storage volume, the initial inflow rate, and the inflow rate at the end of the time step (Eqn. 7.9)

$$\overline{k} = \frac{k(q_{in}(t_0)) + k(q_{in}(t_0 + \Delta t)) + k(v(t_0))}{3} \quad (7.9)$$

with all k values taken from the $\Delta v / \Delta q$ relation (Eqn. 7.7).

To apply Eqns. 7.5 and 7.9, the inflow rates corresponding to the begin and the end of a time step, $q_{in}(t_0)$ and $q_{in}(t_0 + \Delta t)$, must be known.

Inflow rates

Problems with conservation of mass may arise from using $q_{in}(t_0)$ and $q_{in}(t_0 + \Delta t)$ together with the assumption of a linear variation over Δt when simulating multiple reaches in series. This is due to the fact that the outflow from a reach – and thus the inflow of the downstream reach – varies exponentially rather than linearly (see Eqn. 7.3 & 7.5). To allow for a proper mass balance (priority) while also taking into account the variation in the inflow rate (secondary objective), the model uses as input

1. the rate at the end of the time step, $q_{in}(t_0 + \Delta t)$.

2. the average inflow rate for the time step, $\overline{q_{in}}$.

Then, the inflow rate at the begin of the time step, $q_{in}(t_0)$ is estimated from these two values using

$$q_{in}(t_0) = max(0., 2 \cdot \overline{q_{in}} - q_{in}(t_0 + \Delta t))$$

and subsequently applying the correction

$$q_{in}(t_0 + \Delta t) = 2 \cdot \overline{q_{in}} - q_{in}(t_0)$$

The latter correction is necessary to account for the mass balance in those cases where the 2nd argument of $max()$ is negative and $q_{in}(t_0)$ is therefor set to zero. These are cases where the value of the average inflow rate is incompatible with the assumption of a linear variation over Δt.

Outflow rates

Using the concept of the linear reservoir, the outflow rate at the end of the time step is computed from Eqn. 7.10.

$$q_{out}(t_0 + \Delta t) = \frac{1}{\overline{k}} \cdot v(t_0 + \Delta t) \quad (7.10)$$

The time-step averaged outflow rate is calculated using Eqn. 7.11, which is a discrete version of the mass balance equation.

$$\overline{q_{out}} = \frac{v(t_0) - v(t_0 + \Delta t)}{\Delta t} + \overline{q_{in}} \quad (7.11)$$

7.2.3   Hints for application

In hydrological catchment modeling, data on the geometry of river cross-sections are usually scarce. The **topocatch** software (Kneis, 2012a) contains methods to estimate the x-section characteristics for all reaches in a river basin using survey data from a limited number of sites only. Basically, these methods perform a spatial regionalization of the functions $A(h)$ and $R(h)$. It then applies Eqn. 7.8 to generate a table of corresponding storage volumes and outflow rates, allowing for look-up of the retention constant (Eqn. 7.7).

Chapter 8

Evaporation from Water Surfaces

8.1 Introduction

This chapter introduces evaporation models. The approach(es) can be used to estimate the water losses associated with evaporation from lake, reservoir, and river surfaces.

8.2 Makkink model

The Makkink model is a simple empirical equation to estimate evaporation using a minimum set of input data, namely short wave radiation and air temperature. In has been derived for the Netherlands. Using convenient units, the basic equation is (Eqn. 8.1)

$$ e = c \cdot \frac{s}{s + \gamma} \cdot \frac{R_{inS}}{1000 \cdot E_{wat} \cdot \rho_w} + b \qquad (8.1) $$

with

e	Makkink reference evaporation (m/s)
s	Slope of the curve of saturation water vapor pressure (kPa / K)
γ	Psychrometric constant (kPa / K)
R_{inS}	Incoming short-wave radiation (W/m^2)
E_{wat}	Latent heat of water evaporation (kJ/kg).
ρ_w	Density of water (≈ 1000 kg/m^3).
c	Empirical factor (–).
b	Empirical correction term (m/s).

One should realize that only the incoming short-wave radiation is used in Eqn. 8.1, thus other terms of the energy balance, such as reflection (albedo), long wave emissions, and heat storage are all neglected.

For the dimensionless term $s/(s + \gamma)$ Yao (2009) present a convenient approximation based on the air temperature TA in units of °C (Eqn. 8.2). The error from using this approximation is ¡ 4 % for temperatures

Table 8.1: *Makkink evaporation (mm/day) for different values of temperature (°C) and daily-average short-wave radiation (W/m^2). The empirical parameters were set to $c = 0.61$ and $b = -0.012/100/86400$.*

Radiation (W/m²)	Temperature (°C)					
	5	**10**	**15**	**20**	**25**	**30**
50	0.40	0.47	0.53	0.59	0.66	0.72
100	0.93	1.05	1.18	1.31	1.43	1.56
150	1.45	1.64	1.83	2.02	2.21	2.41
200	1.98	2.23	2.48	2.73	2.99	3.25

between 4 and 30 °C and about 7 % at 0 °C when compared to the equations for separate estimation of s and γ given in Hiemstra and Sluiter (2011).

$$ \frac{s}{s + \gamma} \approx 0.439 + 0.01124 \cdot TA \qquad (8.2) $$

The latent heat of water evaporation E_{wat} (kJ/kg) can be estimated from the water temperature T (°C) using Eqn. 8.3 (Hiemstra and Sluiter, 2011). Since water temperature data are usually unavailable, the air temperature TA must be used as a substitute for T.

$$ E_{wat} = 2501 - 2.375 \cdot T \qquad (8.3) $$

For the two empirical parameters, Winter et al. (1995) report values of $c = 0.61$ and $b = -0.012/100/86400$ (unit of b converted from cm/d to m/s). Hiemstra and Sluiter (2011) suggest $c = 0.65$ and $b = 0$ but their report does not explicitly focus on evaporation from water surfaces.

Table 8.1 provides some results of the application of Eqn. 8.1 for selected temperatures and short-wave radiation inputs.

Chapter 9

Evapotranspiration

9.1 Introduction

This chapter describes approaches to model evapotranspiration. The focus is on very simple approaches relying on a two-step calculation procedure:

1. Computation of a *potential* evapotranspiration rate et_{pot}. This represents the maximum possible rate in the absence of water stress. It is basically limited by energy supply.

2. Estimation of the *actual* evapotranspiration rate et_{real} from the potential rate taking into account the properties of vegetation and the limitation by a soil moisture deficit.

9.2 Potential evapotranspiration

9.3 Hargreaves model

This is a very simply model yielding estimates of et_{pot} with daily resolution. It requires as input

- Incoming short-wave radiation

- Daily minimum and maximum temperature

If the radiation is given as a daily average value (instead of a sum), the Hargreaves model takes the form of Eqn. 9.1

$$et_{pot} = CH \cdot \left(\frac{t_{max} + t_{min}}{2} + CT \right) \cdot \tag{9.1}$$

$$\sqrt{t_{max} - t_{min}} \cdot 0.0864 \cdot R_{inS}$$

with

et_{pot}	Hargreaves potential evapotranspiration rate (mm/day)
t_{max}, t_{min}	Daily minimum and maximum of air temperature (°C)
R_{inS}	Daily average of incoming short-wave radiation (W/m^2)
0.0864	Factor to convert R_{inS} from W/m^2 into MJ/m^2/day
CH	Empirical coefficient, CH= 0.0023
CT	Empirical coefficient, CT= 17.8

9.4 Makkink model

The Makkink model is another simple approach to estimate potential evaporation using only temperature and downward short-wave radiation as predictors. The approach is discussed in detail by de Bruin (1987); Feddes (1987); Hiemstra and Sluiter (2011).

Using convenient units, the basic equation without an additive empirical constant (see de Bruin, 1987) is Eqn. 9.2

$$et_{pot} = c \cdot \frac{s}{s + \gamma} \cdot \frac{R_{inS}}{1000 \cdot E_{wat} \cdot \rho_w} \tag{9.2}$$

with

et_{pot}	Makkink reference crop-evaporation (m/s)
s	Slope of the curve of saturation water vapor pressure (kPa / K)
γ	Psychrometric constant (kPa / K)
R_{inS}	Incoming short-wave radiation (W/m^2)
E_{wat}	Latent heat of water evaporation (kJ/kg)
ρ_w	Density of water (≈ 1000 kg/m^3)
1000	Factor to convert kJ into J
c	Dimensionless empirical constant, c=0.65

The latent heat of water evaporation E_{wat} (kJ/kg) is simply a function of temperature (see Eqn. 8.3 on page 55). For the dimensionless term $s/(s + \gamma)$ Yao (2009) present a convenient approximation based on the air temperature (see Eqn. 8.2 on page 55). A more accurate estimate is obtained, however, using the empirical expressions for s and γ (both in hPa/K) from Eqn. 9.3 and Eqn. 9.4

$$s = 6.11 \cdot exp\left(\frac{17.3 \cdot TA}{237.3 + TA}\right) \cdot \qquad (9.3)$$

$$\frac{4105.3}{(237.3 + TA)^2}$$

$$\gamma = 0.016286 \cdot \frac{PA}{E_{wat}(TA)} \qquad (9.4)$$

where PA is the air pressure (hPa) and TA is the air temperature in °C (Dyck and Peschke, 1995).

9.5   Real evapotranspiration

In the approaches described here, the rate of real evapotranspiration et_{real} is computed by multiplying the potential rate et_{pot} with dimensionless correction factors. Typically, these factors account for

- the different transpiration characteristics of the actual vegetation as compared to the reference vegetation to which et_{pot} refers (usually short grass). These factors are known as *crop factors* (Sec. 9.5.1).

- the reduction of plant transpiration due to soil moisture limitation (Sec. 9.5.2).

9.5.1   Crop factors

For some equations to estimate et_{pot}, an extensive set of crop factors has been established based on empirical research. The values vary between different crops and also account for the different stages of plant grow, i. e. seasonality. For the Makkink model (Sec. 9.4), crop factors can be found in Feddes (1987). For wider applicability, it is desireable to derive the crop factors from other easily available data. A potential candidate is the leaf-area index LAI. Based on figure Fig. 9.1,
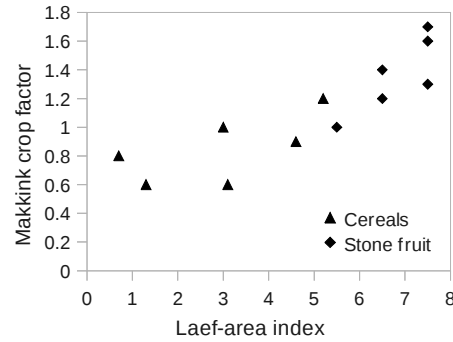
Figure 9.1: *Relation between the crop factor (for Makkink model) and the leaf-area index (m^2/m^2) for two selected crops. Crop factors and the corresponding values of LAI were taken from Feddes (1987) and Ludwig and Bremicker (2006), respectively.*

an approximate relation between the crop factor of the Makkink model and the LAI can be derived (Eqn. 9.5).

$$\text{crop factor} \approx 0.14 \cdot LAI + 0.4 \qquad (9.5)$$

Note that, following the conventional definition of et_{pot}, the crop factor should take a value of one for the reference crop (typically actively growing gras of 12 cm height with unlimited water supply). Assuming that the corresponding LAI is about 5 (see, e. g. Misra and Misra, 1981) or (Bremicker et al., 2006, page 11), the simplest linear approach would be Eqn. 9.6.

$$\text{crop factor} \approx 0.2 \cdot LAI \qquad (9.6)$$

This equation, however, implies that evapotranspiration from bare soil is zero. In reality, a non-zero intercept is more plausible.

During calibration of a hydrological model for the Upper Neckar Basin (Germany), the relation shown in Eqn. 9.7 was identified. It yielded the best result for a larger part of the catchment (gage Kirchtellinsfurt, 2300 km^2). The optimum parameters for smaller sub-basins were similar. The assumed LAI of grassland vegetation in that model was 5.

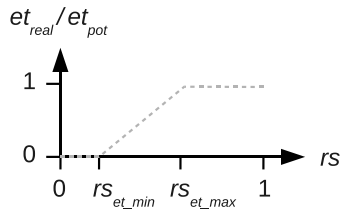$$\text{crop factor} \approx 0.16 \cdot LAI + 0.2 \qquad (9.7)$$

Figure 9.2: *Ratio of real to potential evapotranspiration et_{real}/et_{pot} as a function of relative soil saturation rs.*

9.5.2   Influence of soil moisture

A widely used scheme to account for the limitation of real evapotranspiration by soil moisture is illustrated in Fig. 9.2. This approach uses two empirical constants rs_{etmin} and rs_{etmax} representing threshold values of relative soil saturation. For very dry soil with relative saturation between 0 and rs_{etmin}, real evapotranspiration is zero. For wet conditions with relative saturation between rs_{etmax} and 1, the rate of real evapotranspiration et_{real} is equal to the potential rate et_{pot}. For intermediate conditions, et_{real} is assumed to vary linearly with soil saturation (i. e. soil moisture). Mathematically, this is expressed by Eqn. 9.8.

$$\frac{et_{real}}{et_{pot}} = min\left(1, max\left(0, \frac{rs - rs_{etmin}}{rs_{etmax} - rs_{etmin}}\right)\right)$$

(9.8)

In this definition, the relative soil saturation rs is the quotient of the current soil water content θ and the soil-specific maximum value θ_{max}. Thus, the two parameters rs_{etmin} and rs_{etmax} take values in range 0 to 1. A reasonable estimate for rs_{etmin} can be obtained from data on the water content at the wilting point. This value varies considerably between soil types as illustrated in Fig. 9.3.

Some characteristic values of soil water content (based on Fig. 9.3) and the corresponding estimates of model parameters are presented in Table 9.1.
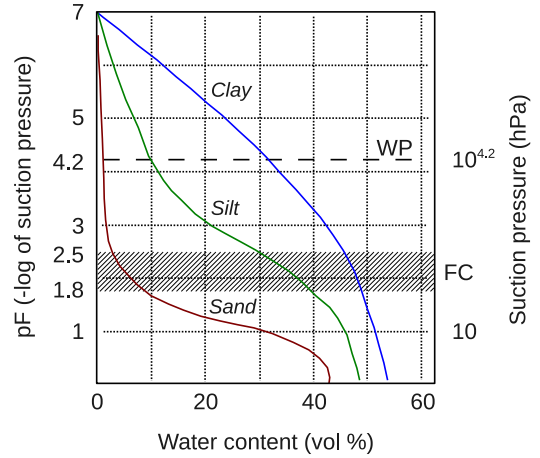
Figure 9.3: *Typical relation between water content and suction pressure for different soil types. The permanent wilting point is defined as pF=4.2 ($\approx$ 1500 kPa). The hatching marks the typical range of the field capacity found in soils. Adapted from Scheffer and Schachtschabel (1998).*

Table 9.1: *Characteristic values of the soil water content θ and corresponding estimates of model parameters derived from Fig. 9.3.*

Soil	θ_{max}	θ at pF=2.5	θ at pF=4.2	rs_{etmax}	rs_{etmin}
Sand	0.43	0.03	0.02	¡ 0.07	0.05
Silt	0.48	0.3	0.1	¡ 0.63	0.21
Clay	0.53	0.46	0.32	¡ 0.86	0.6

Chapter 10

Storage in lakes and reservoirs

10.1 Introduction

This chapter desribes approaches to the simulation of water storage in reservoirs. In a wider sense, the term *reservoir* includes natural lakes and the various types of operated reservoirs.

10.2 Storage in uncontrolled lakes

10.2.1 Processes and equations

The fundamental principle for the simulation of lake storage is expressed by the mass balance equation (Eqn. 10.1).

$$\frac{dv}{dt} = q_{in} + p - q_{out} - e \qquad (10.1)$$

v	Storage volume	L^3
q_{in}	Inflow rate	L^3/T
q_{out}	Outflow rate	L^3/T
p	Precipitation flux	L^3/T
e	Evaporation flux	L^3/T

For a natural lake with a single outflow, the outflow rate is related to the lake's water level h through a rating curve $Q_{out}(h)$ (Fig. 10.1). Furthermore, the water level h is related to the storage volume v by the storage curve $H(v)$. The latter represents the lake's bathymetry, i. e. the topography of the bottom. Sometimes, the rating curve and the storage curve may be represented by analytical functions, typically using power equations or polynomials, respectively. In practice, however, lookup tables generally allow for greater flexibility as compared to analytical expressions.

The rates of precipitation and evaporation fluxes are obtained by multiplying the corresponding rates (di-
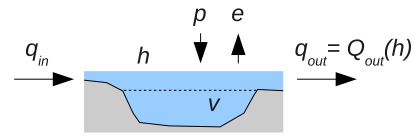
Figure 10.1: *Side view of a lake with uncontrolled outflow through an outlet channel. Symbols as in Eqn. 10.1.*

mension L/T) with an appropriate value of the lake's surface area (Eqn. 10.2 & 10.3).

$$p = P \cdot a_{max} \qquad (10.2)$$

$$e = E \cdot A(H(v)) \qquad (10.3)$$

P	Intensity of precipitation	L/T
E	Rate of evaporation	L/T
a_{max}	Maximum extent of the lake's surface area	L^2
$A(h)$	Surface area as a function of water level h	L^2

The reasons for using different values of the surface area in the calculation of precipitation and evaporation fluxes are as follows:

- If a constant surface area would be used in Eqn. 10.3, this would no longer be a continuous function. As long as the there was some water in the lake, the evaporation flux would be > 0. But as soon as the last amount of liquid water has vanished, the flux becomes zero. Such a discontinuity is problematic when solving the differential equation Eqn. 10.1. The choice of a *continuous* function $A(h)$ resolves this problem, as it makes the evaporation flux E decrease gradually, as the storage volume approaches zero.

- In reality, the lake's surface area being exposed to precipitation is variable too, as expressed by $A(h)$. However, in hydrological catchment models, the area of *land surfaces* is typically constant. Therefore, to avoid mass balance errors, the lake's surface area is taken as constant too. The maximum extent of the lake a_{max} is a natural choice. Effectively, rain falling on possibly dry parts of the bottom still contributes to the lake's storage volume.

Using the rating curve $Q_{out}(h)$ and the storage curve $H(v)$ as well as the definitions from Eqn. 10.2 and 10.3, the mass balance (Eqn. 10.1) can be rewritten as Eqn. 10.4.

$$\frac{dv}{dt} = q_{in} + P \cdot a_{max} - Q_{out}(H(v)) - E \cdot A(H(v))$$

(10.4)

10.2.2　Mathematical solution

Strategy

The two functions $Q_{out}(H(v))$ and $A(H(v))$ at the right hand side of Eqn. 10.4 may be arbitrarily complicated. Moreover, the functions are typically available as lookup tables rather than analytical expressions. Therefore, Eqn. 10.4 has to be solved numerically. To obtain accurate and stable (i. e. positive) solutions, an ODE solver with automatic time-step adjustment must be used.

Inflow rates

The currently used implementation allows for a linear variation of the inflow rate within a discrete modeling time step of length Δt. As input, the time-step averaged inflow rate $\overline{q_{in}}$ and the instantaneous rate at the end of the time step $q_{in}(t_0 + \Delta t)$ are used. The missing rate at the begin of the time step $q_{in}(t_0)$ is estimated as described in Sec. 7.2.2 (page 53).

Outflow rates

The numerical solution of Eqn. 10.4 yields the storage volume at the end of a modeling time step and the corresponding outflow rate $q_{out}(t_0 + \Delta t)$ is obtained from the combined rating curve and storage curve $Q_{out}(H(v))$.

An accurate time-step averaged outflow rate $\overline{q_{out}}$ is calculated from a discrete version of the mass balance equation (Eqn. 10.5).

$$\overline{q_{out}} = \frac{v(t_0) - v(t_0 + \Delta t)}{\Delta t} + \overline{q_{in}} + \frac{vp}{\Delta t} - \frac{ve}{\Delta t} \quad (10.5)$$

Here, vp and ve represent the total volumes of precipitation input and evaporation losses within a single time step, respectively. Both vp and ve are treated as state variables which are initialized to zero at the beginning of a time step (t_0). This approach allows for the computation of a proper mass balance even if the rates of precipitation or evaporation are variable over Δt. Currently, this is only the case for evaporation, since the flux is dependend on the storage (see Eqn. 10.3).

10.2.3　Implementation

Table 10.1 relates the identifier names used in the model implementation (names of state variables, parameters, inputs, and outputs) to the symbols used in the process equations (Sec. 10.2.1). Note that this table does not list external input variables used in the calculation of the rate of evaporation (symbol E in Eqn. 10.3). Modeling concepts for evaporation can be found in Chap. 8.

10.3　Notes on input data

In real-world model applications, the required functions $H(v)$, $Q_{out}(h)$, and $A(h)$ are often not known but have to be estimated. Some recommendations are given in the sub-sections below.

10.3.1　Storage curve

Sometimes, information on the lake's bathymetry are available from topographic maps as lines of equal depth. Via the steps of digitizing and vector-to-raster conversion, a digital elevation model (DEM) of the lake's bottom can be obtained using GIS. Alternatively, the DEM can be obtained by interpolation of punctual measurements. The inverse of the storage curve $H(v)$ can be calculated using Eqn. 10.6.

$$V(h) = (\Delta x)^2 \cdot \sum_{i=1}^{nx} \sum_{k=1}^{ny} max(0, h - z(i,k)) \quad (10.6)$$

Table 10.1: *Symbols used in the process equations (Sec. 10.2.1) and corresponding identifiers.*

Symbol	Identifier	Units	Details
		State variables	
v	v	m^3	Storage volume
vp	vp	m^3	Total volume of precipitation in a single time step
ve	ve	m^3	Total evaporated volume in a single time step
		Simulated inputs	
$\overline{q_{in}}$	qi_avg	m^3/s	Inflow rate (time-step average)
$q_{in}(t_0 + \Delta t)$	qi_end	m^3/s	Inflow rate (value at end of time-step)
		Scalar parameters (object-specific)	
a_{max}	area_max	m^2	Maximum surface area
		Parameter functions (object-specific)	
$H(v)$	v2h	m	Storage curve (tabulated function)
$A(h)$	h2a	m^2	Area curve to compute evaporation loss (tabulated function)
$Q_{out}(h)$	h2q	m^2	Rating curve at lake outlet (tabulated function)
		Outputs	
$\overline{q_{out}}$	qx_avg	m^3/s	Outflow rate (time-step average)
$q_{out}(t_0 + \Delta t)$	qx_end	m^3/s	Outflow rate (value at end of time-step)
h	h	m	Water level

$V(h)$	Storage volume corresponding to water level h	L^3
$(\Delta x)^2$	Area of a single raster cell	L^2
nx, ny	Number of cells in x- and y-direction (grid dimensions)	–
$z(i,k)$	Elevation of the bottom at cell with indices i and k	L

The evaluation of Eqn. 10.6 for discrete values of h yields a lookup table for $V(h)$. The desired function $H(v)$ is then obtained by inverting $V(h)$. Usually, it makes sense to apply some kind of interpolation in order to tabulate $H(v)$ for a reasonable set of arguments v.

For operational model applications, it is important that the table $H(v)$ covers the highest thinkable values of the storage volume v. Otherwise, the model might stop just in the moment where it is needed the most. The choice of a lower limit for v is site-specific. Given that the outflow of the lake never runs dry, it is sufficient if the smallest tabulated value of $H(v)$ corresponds to the lowest point of the channel at the lake's outlet (dashed horizontal line in Fig. 10.1). However, if the water level can fall below this level due to high evaporation (causing the outflow rate to be exactly zero), the table $H(v)$ must also cover those states.

10.3.2   Surface area curve

The function $A(h)$ can be obtained from a DEM as well using Eqn. 10.7. By convention, the logical expression $(h > z(i,k))$ equals 1 if true and it is 0 otherwise.

$$A(h) = (\Delta x)^2 \cdot \sum_{i=1}^{nx} \sum_{k=1}^{ny} (h > z(i,k)) \qquad (10.7)$$

It is sufficient if $A(h)$ is tabulated for the range of h values which are expected to appear during simulation (including extremes). For lakes which can fall dry, it is important that $A(h)$ is continuous, i. e. the value should *gradually* approach zero for values of h which correspond to minimal storage volumes. In other words, the lake's bottom must not be perfectly flat.

10.3.3   Rating curve (uncontrolled lakes)

For natural lakes, the rating curve $Q_{out}(h)$ can be estimated from the characteristics of the outlet channel using Mannings's equation (see Eqn. 7.8 at page 52). The required information include the cross-section's geometry, the slope of the bottom, and the roughness (Manning's n).

For the special case of a channel whose width W is much greater than the flow depth h_{fl}, the hydraulic radius is approximatekly equal to h_{fl}. Then, Mannings's equation simplifies to Eqn. 10.8.

$$q(h_{fl}) = \frac{1}{n} \cdot \sqrt{S_f} \cdot h_{fl}^{5/3} \cdot W \qquad (10.8)$$

q	Flow rate	m^3/s
S_f	Slope of the energy grade line	–
h_{fl}	Flow depth (x-section average)	m
W	Channel width	m
n	Manning's n (parameter)	Non-physical

List of Figures

List of Tables

Bibliography

Bremicker, M., Homagk, P., Ludwig, K., 2006. Hochwasserfrühwarnung und Hochwasservorhersage in Baden-Württemberg. Wasserwirtschaft Jg. 96, Nr. 7-8, 46–50.

de Bruin, H.A.R., 1987. From Penman to Makkink, in: Hooghart, J.C. (Ed.), Evaporation and Weather: Proceedings and information No. 39, TNO Committee on Hydrological Research, The Hague.

Dyck, S., Peschke, G., 1995. Grundlagen der Hydrologie. Verlag für Bauwesen.

Feddes, R.A., 1987. Crop factors in relation to Makkink reference-crop evapotranspiration, in: Hooghart, J.C. (Ed.), Evaporation and Weather: Proceedings and information No. 39, TNO Committee on Hydrological Research, The Hague.

Hiemstra, P., Sluiter, R., 2011. Interpolation of Makkink evaporation in the Netherlands. Technical Report TR-327. Royal Netherlands Meteorological Institute. De Bilt.

Hock, R., 2005. Glacier melt: A review of processes and their modelling. Progress in Physical Geography 29, 362–391.

Illangasekare, T.H., Walter, R.J., Meier, M.F., Pfeffer, W.T., 1990. Modeling of meltwater infiltration in subfreezing snow. Water ressources research 26, 1001–1012.

Kirpich, Z.P., 1940. Time of concentration of small agricultural watersheds. Civil Engineering 10, 362.

Knauf, D., 1980. Analyse und Berechnung oberirdischer Abflüsse. Verlag Paul Parey. volume 46 of *Schriftenreihe des DVWK*. chapter Berechnung des Abflusses aus einer Schneedecke. pp. 45–135.

Kneis, D., 2012a. Eco-Hydrological Simulation Environment (ECHSE) - Documentation of Pre- and Post-Processors. University of Potsdam, Institute of Earth- and Environmental Sciences. URL: http://echse.bitbucket.org/downloads/documentation/echse_tools_doc.pdf.

Kneis, D., 2012b. Eco-Hydrological Simulation Environment (ECHSE) - Documentation of the Generic Components. University of Potsdam, Institute of Earth- and Environmental Sciences. URL: http://echse.bitbucket.org/downloads/documentation/echse_core_doc.pdf.

Ludwig, K., Bremicker, M. (Eds.), 2006. The water balance model LARSIM - Design, content and application. volume 22 of *Freiburger Schriften zur Hydrologie*. University of Freiburg, Institute of Hydrology.

Male, D.H., Gray, D.M. (Eds.), 1981. Handbook of Snow - Principles, Processes, Management and Use. Pergammon Press. chapter Snowcover Ablation and Runoff. pp. 360–436.

Misra, M.K., Misra, B.N., 1981. Seasonal changes in leaf area index and chlorophyll in an indian grassland. Journal of Ecology 69, 797–805.

Morris, E.M., Kelly, R.J., 1990. A theoretical determination of the characteristic equation of snow in the pendular regime. Journal of Glaciology 36, 179–187.

Scheffer, F., Schachtschabel, P. (Eds.), 1998. Lehrbuch der Bodenkunde. Enke.

Tarboton, D.G., Luce, C.H., 1996. Utah Energy Balance Snow Accumulation and Melt Model (UEB). Technical Report. Utah State University and USDA Forest Service.

Todini, E., 1996. The ARNO rainfall-runoff model. Journal of Hydrology 175, 339–382.

Winter, T.C., Rosenberry, D.O., Sturrock, A.M., 1995. Evaluation of 11 equations for determining evaporation from a small lake in the north central united states. Water Resources Research 31, 983–993.

Yao, H., 2009. Long-term study of lake evaporation and evaluation of seven estimation methods: Results from dickie lake, south-central ontario, canada. J. Water Resource and Protection 2, 59–77.

Zhao, R.J., Zuang, Y.L., Fang, L.R., Liu, X.R., Zhang, Q.S., 1980. The Xinanjiang model, in: Hydrological forecasting, Proceedings of the Oxford Symposium, IAHS Press, Wallingford, UK. pp. 351–356.